

ELECTRON TUBES

Volume II

(1942-1948)

ELECTRON TUBES

Volume II

(1942-1948)

Edited by

ALFRED N. GOLDSMITH
ARTHUR F. VAN DYCK
ROBERT S. BURNAP
EDWARD T. DICKEY
GEORGE M. K. BAKER

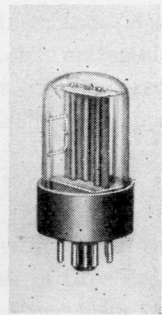
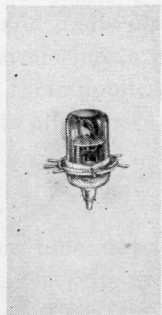
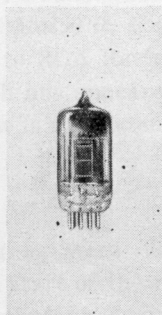
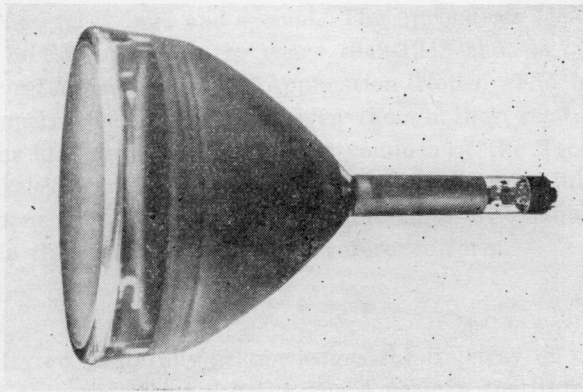
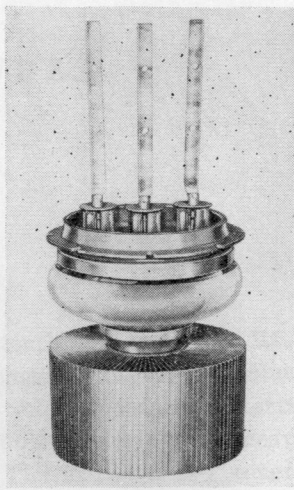
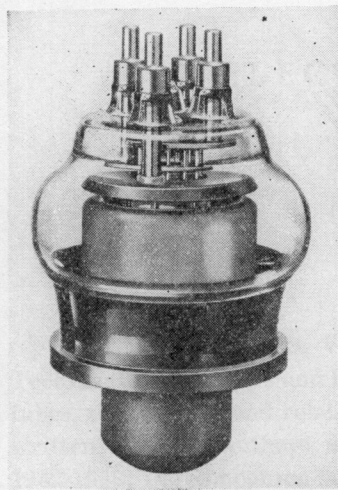
MARCH, 1949

Published by

RCA REVIEW
RADIO CORPORATION OF AMERICA
RCA LABORATORIES DIVISION
Princeton, New Jersey

**Copyright, 1949, by
Radio Corporation of America
RCA Laboratories Division**

Printed in U.S.A.



ELECTRON TUBES OF TODAY

ELECTRON TUBES

Volume II

(1942-1948)

PREFACE

ELECTRON TUBES, Volume II, is the tenth volume in the **RCA Technical Book Series** and the second on the general subject of vacuum tubes, thermionics and related subjects. This volume contains material written by RCA authors and originally published during the years 1942-1948; the companion book, ELECTRON TUBES, Volume I, covers the period 1935-1941.

The papers in this volume are presented in four sections: general; transmitting; receiving; and special. The appendices include an electron tube bibliography for the years 1942-1948 and, as an additional source of reference, a list of Application Notes. The bibliography lists all papers concerning tubes even though they relate to specific applications and are covered in other volumes of the Technical Book Series on television, facsimile, UHF, and frequency modulation. This has been done to insure that all applicable material on tubes would be available in this volume—at least in reference form.

* * *

RCA Review gratefully acknowledges the courtesy of the Institute of Radio Engineers (*Proc. I.R.E.*), the American Institute of Physics (*Jour. Appl. Phys.*, *Jour. Opt. Soc. Amer.*, and *Phys. Rev.*), the Franklin Institute (*Jour. Frank. Inst.*), the Society of Motion Picture Engineers (*Jour. Soc. Mot. Pic. Eng.*), and Radio Magazines, Inc. (*Audio Eng.*) in granting to RCA Review permission to republish material by RCA authors which has appeared in their publications. The appreciation of RCA Review is also extended to all authors whose papers appear herein.

* * *

As outstanding as were electron tube developments from their invention until the start of the recent war, the progress in tube design and application technique during and since the war has been even more remarkable, particularly in power and miniature tubes. Still

newer work has already produced components which lend promise of replacing electron tubes for certain uses, but for the great majority of applications, electron tubes will continue to serve as the framework around which radio-electronic progress will be fashioned.

ELECTRON TUBES, Volume II, like its predecessor is being published, therefore, in the sincere hope that it will serve as a useful reference text and source of basic information to advance radio and electronics in all of its many facets.

The Manager, RCA Review

RCA Laboratories,
Princeton, New Jersey
March 19, 1949

ELECTRON TUBES

Volume II

(1942-1948)

CONTENTS

	PAGE
FRONTISPICE	—v—
PREFACE	—vii—

GENERAL

Analysis of Rectifier Operation	O. H. SCHADE	1
Space-Current Flow in Vacuum-Tube Structures	B. J. THOMPSON	40
The Electron Mechanics of Induction Acceleration	J. A. RAJCHMAN AND W. H. CHERRY	56
The Motion of Electrons Subject to Forces Transverse to a Uniform Magnetic Field	P. K. WEIMER AND A. ROSE	105

Summaries:

Quantum Effects in the Interaction of Electrons with High Frequency Fields and the Transition to Classical Theory	L. P. SMITH	119
Carbide Structures in Carburized Thoriated-Tungsten Filaments	C. W. HORSTING	119
Determination of Current and Dissipation Values for High-Vacuum Rectifier Tubes	A. P. KAUZMANN	120

TRANSMITTING

Grounded-Grid Radio-Frequency Voltage Amplifiers	M. C. JONES	121
Excess Noise in Cavity Magnetrons	R. L. SPROULL	139
The Maximum Efficiency of Reflex-Klystron Oscillators	E. G. LINDER AND R. L. SPROULL	151
A Developmental Pulse Triode for 200 Kw. Output at 600 Mc.	L. S. NERGAARD, D. G. BURNSIDE AND R. P. STONE	171
A New 100-Watt Triode for 1000 Megacycles	W. P. BENNETT, E. A. ESCHBACH, C. E. HALLER AND W. R. KEYE	180
Duplex Tetrode UHF Power Tubes	P. T. SMITH AND H. R. HEGBAR	194

Summaries:

The Design and Development of Three New Ultra-High-Frequency Transmitting Tubes	C. E. HALLER	207
Development of Pulse Triodes and Circuit to Give One Megawatt at 600 Megacycles	R. R. LAW, D. G. BURNSIDE, R. P. STONE AND W. B. WHALLEY	207
Power Measurements of Class B Audio Amplifier Tubes	D. P. HEACOCK	208
Coaxial Tantalum Cylinder Cathode for Continuous-Wave Magnetrons	R. L. JEPSEN	208
Stabilized Magnetron for Beacon Service	J. S. DONAL, JR., C. L. CUCCIA, B. B. BROWN, C. P. VOGEL AND W. J. DODDS	209
A Frequency-Modulated Magnetron for Super-High Frequencies	G. R. KILGORE, C. I. SHULMAN AND J. KURSHAN	210
A 1-Kilowatt Frequency-Modulated Magnetron for 900 Megacycles	J. S. DONAL, JR., R. R. BUSH, C. L. CUCCIA AND H. R. HEGBAR	210

CONTENTS (*Continued*)

RECEIVING

	PAGE
The Operation of Frequency Converters and Mixers for Superheterodyne Reception	E. W. HEROLD
Beam-Deflection Control for Amplifier Tubes	G. R. KILGORE
Some Notes on Noise Theory and Its Application to Input Circuit Design	W. A. HARRIS
	280

Summaries:

Superheterodyne Frequency Conversion Using Phase-Reversal Modulation	E. W. HEROLD
Radio-Frequency Performance of Some Receiving Tubes in Television Circuits	R. M. COHEN
The Transistrol, An Experimental Automatic-Frequency-Control Tube	J. KURSHAN
	294

SPECIAL

A Phototube for Dye Image Sound Track	A. M. GLOVER AND A. R. MOORE
Behavior of a New Blue-Sensitive Phototube in Theater Sound Equipment	J. D. PHYFE
An Infrared Image Tube and Its Military Applications	G. A. MORTON AND L. E. FLORY
Multiplier Photo-Tube Characteristics: Application to Low Light Levels	R. W. ENGSTROM
Small-Signal Analysis of Traveling-Wave Tube	C. I. SHULMAN AND M. S. HEAGY
Barrier Grid Storage Tube and Its Operation	A. S. JENSEN, J. P. SMITH, M. H. MESNER AND L. E. FLORY
The Brightness Intensifier	G. A. MORTON, J. E. RUEDY AND G. L. KRIEGER
Analysis of a Simple Model of Two-Beam Growing-Wave Tube	L. S. NERGAARD
	408
	422

Summaries:

Luminescence and Tenebrescence as Applied in Radar	H. W. LEVERENZ
A Newly Developed Light Modulator for Sound Recording	G. L. DIMMICK
The Behavior of "Magnetic" Electron Multipliers as a Function of Frequency	L. MALTER
Performance Characteristics of Long-Persistence Cathode-Ray Tube Screens; Their Measurement and Control	R. E. JOHNSON AND A. E. HARDY
The Storage Orthicon and Its Application to Telera	S. V. FORGUE
Electron Tube Phonograph Pickup	H. F. OLSON AND J. PRESTON
Performance of 931-A Type Multiplier in a Scintillation Counter	G. A. MORTON AND J. A. MITCHELL
	441
	442
	442
	443

APPENDIX I—ELECTRON TUBE BIBLIOGRAPHY (1942-1948)	444
APPENDIX II—LIST OF APPLICATION NOTES (1947-1948)	454

ANALYSIS OF RECTIFIER OPERATION*†

BY

O. H. SCHADE

Tube Department, RCA Victor Division,
Harrison, N. J.

Summary—An analysis of rectifier operation in principal circuits is made. The introduction of linear equivalent diode resistance values permits a simplified and accurate treatment of circuits containing high-vacuum diodes and series resistance. The evaluation of these equivalent resistance values and a discussion of emission characteristics of oxide-coated cathodes precede the circuit analysis.

Generalized curve families for three principal condenser-input circuits are given to permit the rapid solution of rectifier problems in practical circuits without inaccuracies due to idealizing assumptions.

The data presented in this paper have been derived on the basis of a sinusoidal voltage source. It is apparent that the graphic analysis may be applied to circuits with nonsinusoidal voltage sources or intermittent pulse waves.

It is also permissible to consider only the wave section during conduction time and alter the remaining wave form at will. Complicated wave shapes may thus be replaced in many cases by a substantially sinusoidal voltage of higher frequency and intermittent occurrence as indicated by shape and duration of the highest voltage peak.

The applications of these principles have often explained large discrepancies from expected results as being caused by series or diode resistance and excessive peak-current demands.

Practical experience over many years has proved the correctness and accuracy of the generalized characteristics of condenser-input circuits.

INTRODUCTION

RECTIFIER circuits, especially of the condenser-input type, are extensively used in radio and television circuits to produce unidirectional current and voltages. The design of power supplies, grid-current bias circuits, peak voltmeters, detectors and many other circuits in practical equipment is often based on the assumption that rectifier- and power-source resistance are zero, this assumption resulting in serious errors. The rectifier element or diode, furthermore has certain peak-current and power ratings which should not be exceeded. These values vary considerably with the series resistance of the circuit.

General operating characteristics of practical rectifier circuits have been evaluated and used by the writer for design purposes and informa-

† Reprinted from *Proc. I.R.E.*, July, 1943.

* Decimal Classification: R337 X R356.3.

tion since early 1934, but circumstances have delayed publication. Several papers¹⁻⁴ have appeared in the meantime treating one or another part of the subject on the assumption of zero series resistance. Practical circuits have resistance and may even require insertion of additional resistance to protect the diode and input condenser against destructive currents. The equivalent diode resistance and the emission from oxide-coated cathodes are, therefore, discussed preceding the general circuit analysis. This analysis is illustrated on graphic constructions establishing a direct link with oscillograph observations on practical circuits. A detailed mathematical discussion requires much space and is dispensed with in favor of graphic solutions, supplemented by generalized operating characteristics.

I. PRINCIPLES OF RECTIFICATION

General

Rectification is a process of synchronized switching. The basic rectifier circuit consists of one synchronized switch in series with a single-phase source of single frequency and a resistance load. The switch connection between load terminals and source is closed when source and load terminals have the same polarity, and is open during the time of opposite polarity. The load current consists of half-wave pulses. This simple circuit is unsuitable for most practical purposes, because it does not furnish a smooth load current.

The current may be smoothed by two methods: (a) by increasing the number of phases, and (b) by inserting reactive elements into the circuit. The phase number is limited to two for radio receivers. The circuit analysis which follows later on will treat single- and double-phase rectifier circuits with reactive circuit elements.

Switching in reactive circuits gives rise to "transients." Current and voltage cannot, therefore, be computed according to steady-state methods.

The diode functions as a self-timing electronic switch. It closes the circuit when the plate becomes positive with respect to the cathode

¹ M. B. Stout, "Analysis of rectifier filter circuits," *Elec. Eng. Trans. A.I.E.E.* (*Elec. Eng.*, September, 1935), vol. 54, pp. 977-984; September, 1935.

² N. H. Roberts, "The diode as half-wave, full-wave and voltage-doubling rectifier," *Wireless Eng.*, vol. 13, pp. 351-362; July, 1936; and pp. 423-470; August, 1936.

³ J. C. Frommer, "The determination of operating data and allowable ratings of vacuum-tube rectifiers," *Proc. I.R.E.*, vol. 29, pp. 481-485; September, 1941.

⁴ D. L. Waidelich, "The full-wave voltage-doubling rectifier circuit," *Proc. I. R. E.*, vol. 29, pp. 554-558; October, 1941.

and opens the circuit at the instant when the plate current becomes zero.

The diode has an internal resistance which is a function of current. When analyzing rectifier circuits, it is convenient to treat the internal resistance of the diode rectifier as an element, separated from the "switch action" of the diode. Fig. 1 illustrates the three circuit elements so obtained and their respective voltage-current characteristics (see Section II). The diode characteristic is the sum of these characteristics. The resistance r_d is effective only when the switch is closed, i.e., during the conduction period of the diode. The effective diode resistance must, therefore, be measured or evaluated within conduction-time limits. Consider a switch in series with a fixed resistance and any number of other circuit elements connected to a battery of fixed voltage. The direct current and root-mean-square current

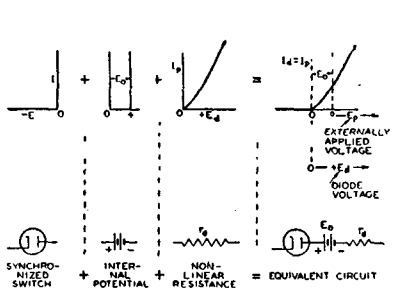


Fig. 1—Characteristics and equivalent circuit for high-vacuum diodes.

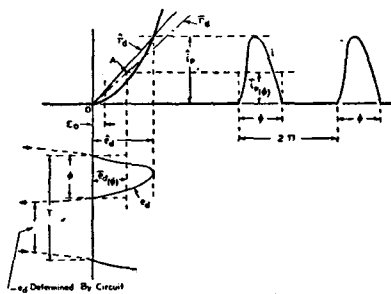


Fig. 2—Graphic evaluation of equivalent diode resistance values.

which flow in this circuit will depend on the time intervals during which the switch is closed and open; the resistance value is not obtainable from these current values and the battery voltage. The correct value is obtained only when the current and voltage drop in the resistance are measured during the time angle ϕ (Fig. 2) when the switch is closed.

The method of analysis of rectifier circuits to be discussed in this paper is based on the principle that the nonlinear effective resistance of the diode may be replaced analytically by an equivalent fixed resistance which will give a diode current equal to that obtained with the actual nonlinear diode resistance. The correct value to be used for the equivalent fixed resistance depends upon whether we are analyzing for peak diode current, average diode current, or root-mean-square diode current.

At the outset of an analysis amplitude and wave shape of the diode current are not known and the diode resistance must, therefore, be determined by successive approximations.

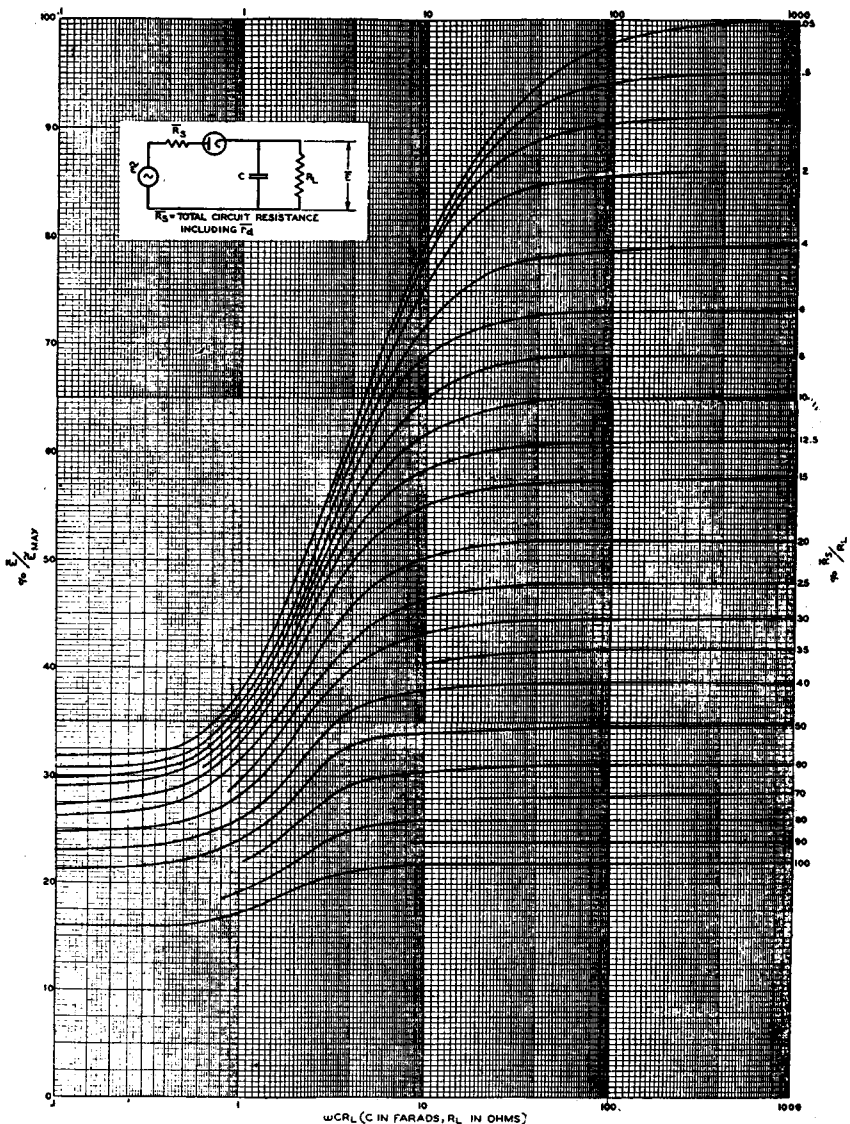


Fig. 3—Relation of applied alternating peak voltage to direct output voltage in half-wave, condenser-input circuits.

The complexity of repeated calculations, especially on condenser-input circuits, requires that the operating characteristics of the circuit be plotted generally as functions of the circuit constants including series resistance in the diode circuit as a parameter.

Data for these plots (such as Figs. 3 to 7) are to be obtained by general analysis of circuits with linear resistances.

The solution of a practical condenser-input-circuit problem requires the use of three different equivalent linear circuits and diode resistance values.

The resistance values are obtainable from the peak current alone because wave shape can be eliminated as a factor by means of a general relation given by (6). The practical analysis of condenser input circuits thus simplified, is carried out as follows:

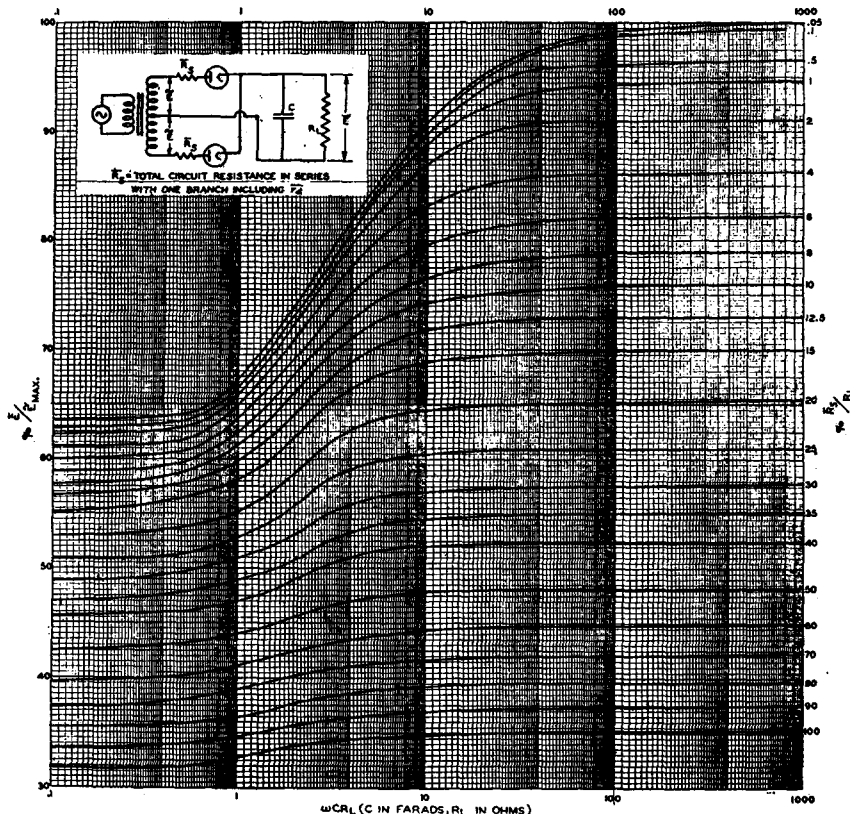


Fig. 4—Relation of applied alternating peak voltage to direct output voltage in full-wave, condenser-input circuits.

The average diode current is estimated roughly and the diode peak current is assumed to be four times the average value. The diode characteristic (Fig. 8) furnishes an initial peak-resistance value and (6) furnishes the other diode resistance values (see R_s values in Fig. 9). Direct output voltage and average current are now obtained with the equivalent average value \bar{R}_s from the respective plot (Figs. 3 to 5) as a first approximation. Another chart (Fig. 6) furnishes the peak-

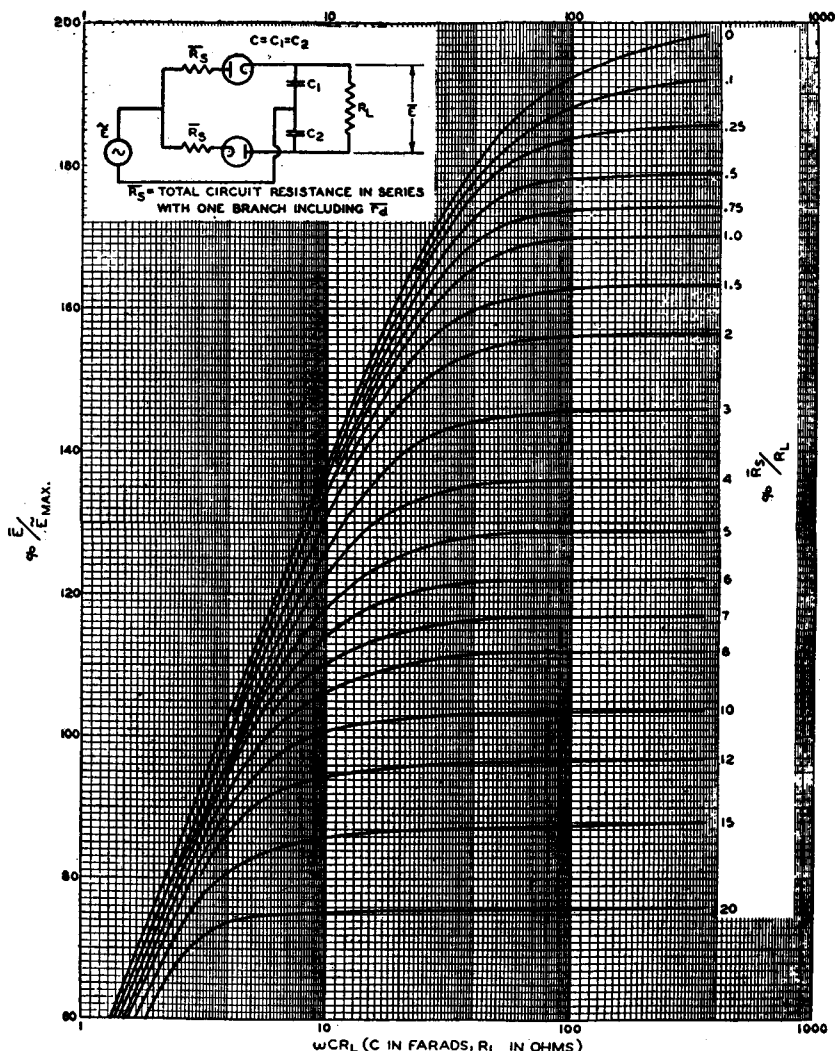


Fig. 5—Relation of applied alternating peak voltage to direct output voltage in condenser-input, voltage-doubling circuits.

to-average-diode-current ratio with the peak value \hat{R}_s , and thus the peak current and diode peak resistance in close approximation.

A second approximation gives usually good agreement between initial and obtained resistance values, which are then used to obtain other operating data.

A theoretical treatment of the method just described will be omitted in favor of an analysis of operating characteristics of the

rectifier tube itself. The user of tubes may welcome information on the subject of peak emission which is of vital importance in the rating and trouble-free operation of any tube with an oxide-coated cathode.

II. ANODE AND CATHODE CHARACTERISTICS OF RECTIFIER TUBES

Anode Characteristics

1. Definitions of Resistance Values

The instantaneous resistance (r_d) of a diode is the ratio of the instantaneous plate voltage e_d to the instantaneous plate current i_p

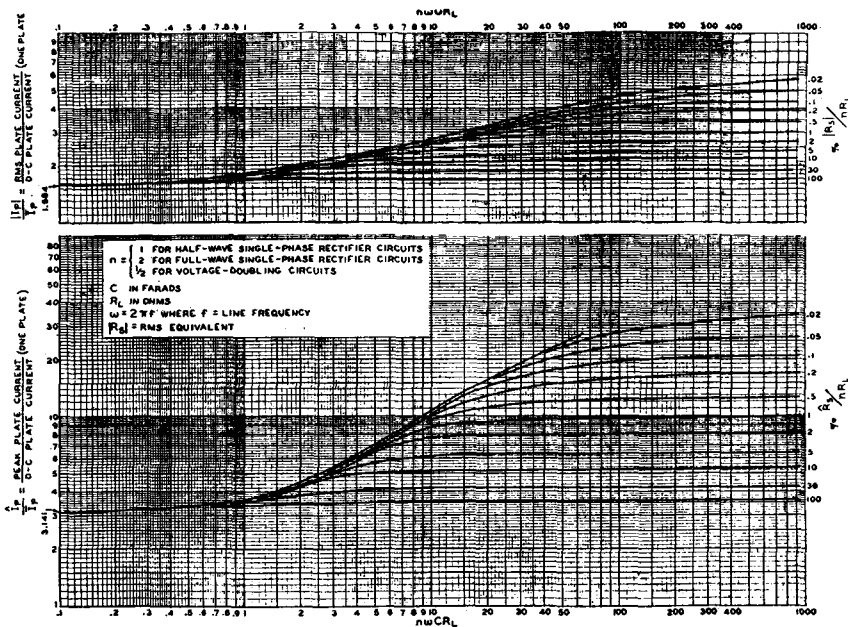


Fig. 6—Relation of peak, average, and root-mean-square diode current in condenser-input circuits.

at any point on the characteristic measured from the operating point (see Fig. 1). It is expressed by

$$r_d = \frac{e_d}{i_p}. \quad (1)$$

The operating point (0) of a diode is a fixed point on the characteristic, marked by beginning and end of the conduction time. It is, therefore, the cutoff point $I_d = 0$ and $E_d = 0$, as shown in Fig. 1. The operating point is independent of the wave form and of the conduction time ϕ (see Fig. 2).

The peak resistance⁵ (\hat{r}_d) is a specific value of the instantaneous resistance and is defined as

$$\hat{r}_d = \frac{\hat{e}_d}{\hat{i}_p} \text{ (see Fig. 2).} \quad (2)$$

Peak voltage \hat{e}_d and peak current \hat{i}_p are measured from the operating point 0.

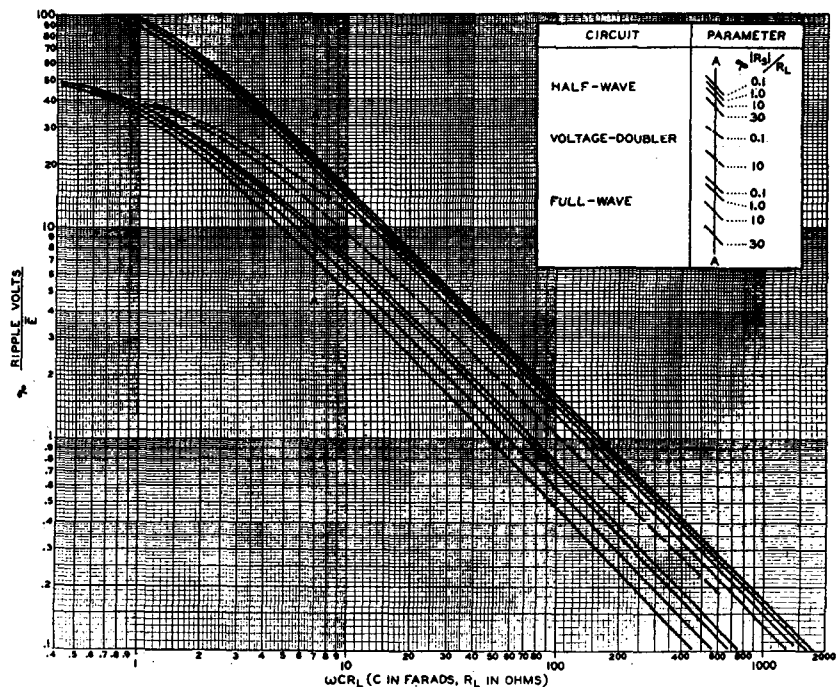


Fig. 7—Root-mean-square ripple voltage of condenser-input circuits.

The equivalent average resistance (\bar{r}_d) is defined on the basis of circuit performance as a resistance value determining the magnitude of the average current in the circuit. The value \bar{r}_d is, therefore, the ratio of the average voltage drop $\bar{e}_{d(\phi)}$ in the diode during conduction time to the average current $\bar{i}_{p(\phi)}$ during conduction time, or

$$\bar{r}_d = \frac{\bar{e}_{d(\phi)}}{\bar{i}_{p(\phi)}}. \quad (3)$$

⁵ For system of symbols, see Appendix.

The curved diode characteristic is thus replaced by an equivalent linear characteristic having the slope \bar{r}_d and intersecting the average point A , as shown in Fig. 2. The co-ordinates $\bar{e}_{d(\phi)}$ and $\bar{i}_{p(\phi)}$ of the average point depend on the shape of voltage and current within the time angle ϕ . The analysis of rectifier circuits shows that the shape of the current pulse in actual circuits varies considerably between different circuit types.

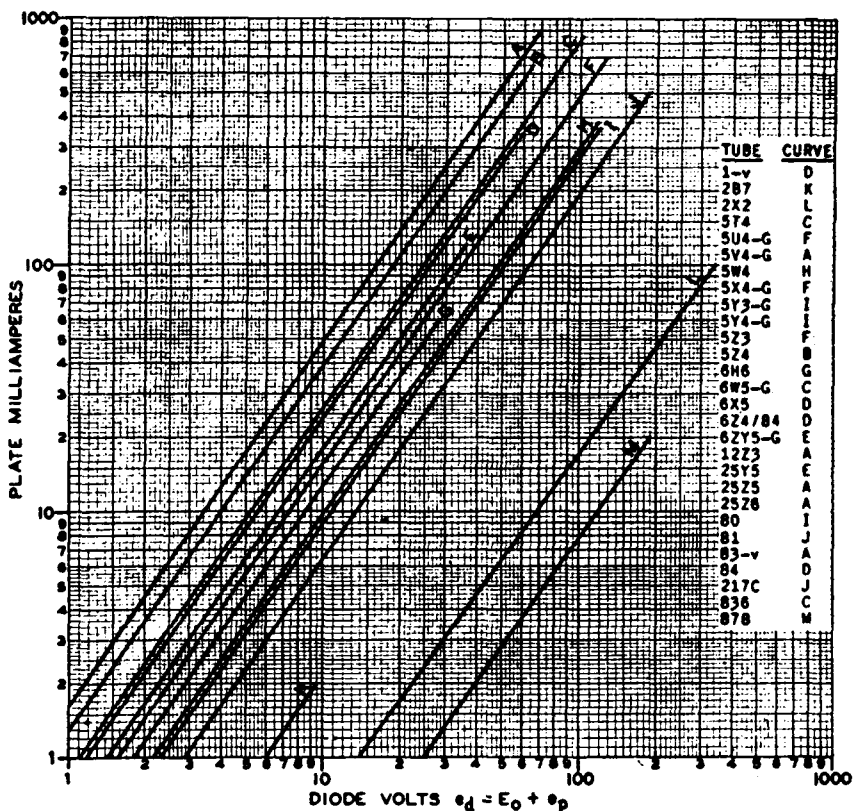
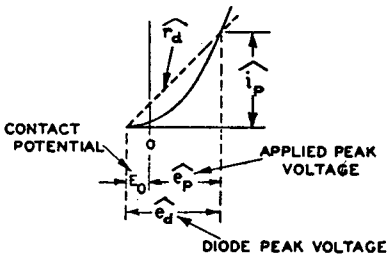
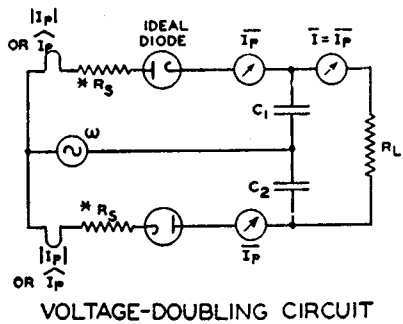
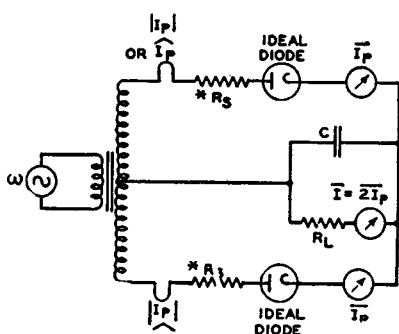
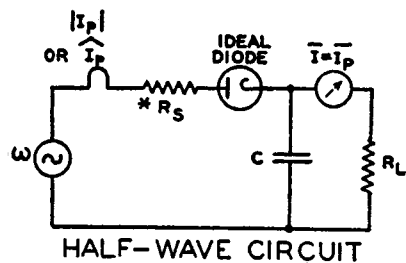


Fig. 8—Average anode characteristics of some RCA rectifier tubes.

The equivalent root-mean-square resistance ($|r_d|$) is defined as the resistance in which the power loss P_d is equal to the plate dissipation of the diode when the same value of root-mean-square current $|I_d|$ flows in the resistance as in the diode circuit. It is expressed by

$$|r_d| = \frac{P_d}{|I_d|^2}. \quad (4)$$



$$\widehat{r_d} = 0.88 \overline{r_d} = 0.935 |r_d| = \frac{\overline{e_d}}{I_P}$$

R_S = EXTERNAL RESISTANCE

$$\widehat{R_S} = R_S + \widehat{r_d}$$

$\widehat{r_d}$ = PEAK DIODE RESISTANCE

$$\overline{R_S} = R_S + \overline{r_d}$$

$\overline{r_d}$ = EQUIVALENT AVE. DIODE RESISTANCE

$$|R_S| = R_S + |r_d|$$

$|r_d|$ = EQUIVALENT R.M.S. DIODE RESISTANCE

* USE $\widehat{R_S}$, $\overline{R_S}$, OR $|R_S|$ AS REQUIRED

Fig. 9—Equivalent circuits and resistance values for condenser-input rectifier circuits.

2. Measurement of Equivalent Diode Resistances

The equivalent resistance values of diodes can be measured by direct substitution under actual operating conditions. The circuit arrangement is shown in Fig. 10. Because the diode under test must be replaced as a whole by an adjustable resistance of known value, a second switch (a mercury-vapor diode identified in the figure as the ideal diode) with negligible resistance must be inserted in order to preserve the switch-action in the circuit.

When a measurement is being made, the resistor R_d is varied until the particular voltage or current under observation remains unchanged for both positions of the switch S . We observe (1) that it is impossible to find one single value of R_d which will duplicate conditions of the

actual tube circuit, i.e., give the same values of peak, average, and root-mean-square current in the circuit; (2) that the ratio of these three "equivalent" resistance values of the diode varies for different combinations of circuit elements; and (3) that the resistance values are functions of the current amplitude and wave shape.

3. Wave Forms and Equivalent Resistance Ratios for Practical Circuit Calculations

The form of the current pulse in practical rectifier circuits is determined by the power factor of the load circuit and the phase number. Practical circuits may be divided into two main groups: (a) circuits with choke-input filter; and (b) circuits with condenser-input filter.

The diode current pulse in choke-input circuits has a rectangular form on which is superimposed one cycle of the lowest ripple frequency. In most practical circuits, this fluctuation is small as compared with the average amplitude of the wave and may be neglected when determining the equivalent diode resistances. It is apparent then that the equivalent diode resistance values are all equal and independent of the type of diode characteristics for square-wave forms. Hence, for choke-input circuits, we have

$$\hat{r}_d = \bar{r}_d = |r_d|. \quad (5)$$

The diode current pulse in condenser-input circuits is the summation of a sine-wave section and a current having an exponential decay. It varies from a triangular form for $\phi < 20$ degrees to a full half cycle ($\phi = 180$ degrees) as the other extreme. In Table I are given the ratios of voltages, currents, and resistance values during conduction time for two principal types of rectifier characteristics: the 3/2-power-law characteristic of high-vacuum diodes, and the idealized rectangular characteristic of hot-cathode, mercury-vapor diodes. In this table, the designation $|i_p|_{(\phi)}$ represents the root-mean-square value of the current during the conduction time.

It follows that the relation

$$\hat{r}_d = 0.88 \bar{r}_d = 0.93 |r_d| \quad (6)$$

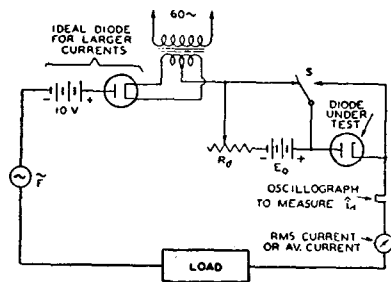


Fig. 10—Circuit for measuring equivalent diode resistance values.

Table I

Conduc- tion Time Angle θ	Wave Shape	3/2-Power Rectifier Characteristic						Rectangular Characteristic		
		$\bar{i}_{p(\phi)}$	$ \bar{i}_p _{(\phi)}$	$\bar{e}_{d(\phi)}$	\bar{r}_d	$ r_d $	$\bar{e}_{d(\phi)}$	\bar{r}_d	$ r_d $	
		\bar{i}_p	\hat{i}_p	\hat{e}_d	\hat{r}_d	\hat{r}_d	\hat{e}_d	\hat{r}_d	\hat{r}_d	
Condenser-Input Circuits										
Degrees ≤ 20		0.500	0.577	0.593	1.185	1.120	1.0	2.00	1.500	
90 and 180		0.637	0.707	0.715	1.120	1.057	1.0	1.57	1.272	
130		0.725	0.780	0.787	1.085	1.030	1.0	1.38	1.190	
Choke-Input Circuits										
180		1.0	1.0	1.0	1.0	1.0	1.0	1.0	1.0	1.0

is representative for the group of condenser-input circuits containing high-vacuum diodes, and holds within ± 5 per cent over the entire range of variation in wave shape. The actual error in circuit calculations is smaller as the diode resistance is only part of the total series resistance in the circuit.

CATHODE CHARACTERISTICS

Peak-Emission and Saturation of Oxide-Coated Cathodes

The normal operating range of diodes (including instantaneous peak values) is below the saturation potential because the plate dissipation rises rapidly to dangerous values if this potential is exceeded. Saturation is definitely recognized in diodes with tungsten or thoriated-tungsten cathodes as it does not depend on the time of measurement, provided the plate dissipation is not excessive. The characteristics of such diodes are single-valued even in the saturated range, i.e., the range in which the same value of current is obtained at a given voltage whether the voltage has been increased or decreased to the particular value.

Diodes with oxide-coated cathodes may have double-valued characteristics because of the coating characteristic. The cathode coating has resistance and capacitance, both of which are a function of temperature, current, and the degree of "activation."

A highly emitting monatomic layer of barium on oxygen is formed on the surface of the coating, which, when heated, supplies the electron cloud forming the space charge above the coating surface (see Fig. 11). The emission from this surface may have values as high as 100 amperes per square centimeter. The flow of such enormous currents is, however, dependent on the internal-coating impedance, and is possible only under certain conditions. Special apparatus is required to permit observation of high current values which, to prevent harm to the tube, can be maintained only over very short time intervals determined by the thermal capacity of the plate and coating. For example, an instantaneous power of 15 kilowatts must be dissipated in the close-spaced diode type 83-v at a current of 25 amperes from its cathode surface of only 1 square centimeter.

Equipment for such observations was built in June, 1937, by the author after data obtained in 1935 on a low-powered curve tracer⁶ indicated the need for equipment having a power source of very low internal impedance for measurements on even relatively small diodes.

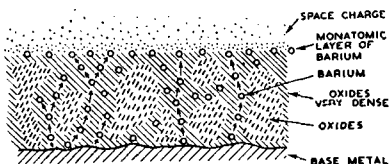


Fig. 11—Representation of cathode coating.

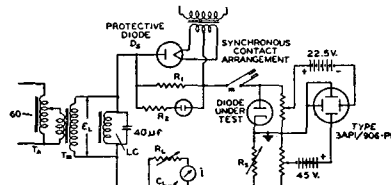


Fig. 12—Peak emission test circuit.

1. Measurement of Diode Characteristics and Peak Emission

The circuit principle is shown in Fig. 12. The secondary voltage of a 2-kilovolt-ampere transformer T_m is adjustable from zero to 2 kilovolts by means of an autotransformer T_A . Transformer and line reactances are eliminated for short-time surge currents by a large condenser load ($C = 20$ to 80 microfarads). The large reactive current is "tuned out" by a choke L of considerable size. The voltage is applied through a large mercury diode and a synchronous contact arrangement m to the tube under test in series with a resistance box R_s and a condenser input load C_L and R_L . This load permits adjustment of the peak-to-average current ratio. Variation of R_L changes the average current. Variation of C_L and phasing of the synchronous contact m with respect to the 60-cycle line voltage permit regulation, within wide limits, of the rate of change and duration of the current pulses.

The dynamic voltage-current characteristic of the tube under test

⁶ Demonstrated, Rochester Fall Meeting, Rochester, N. Y., November 18, 1935.

is observed on a cathode-ray oscilloscope connected in the conventional manner. Calibration deflections are inserted (not shown) by other synchronous contacts to provide accurate and simultaneously visible substitution co-ordinates which may be moved to any point in the characteristic.

The motor-driven synchronous contactor closes the circuit at a desired instant of the line-voltage cycle. The circuit may then be maintained closed for approximately 30 cycles to allow decay of the starting transient (see Fig. 13). It is then opened for approximately

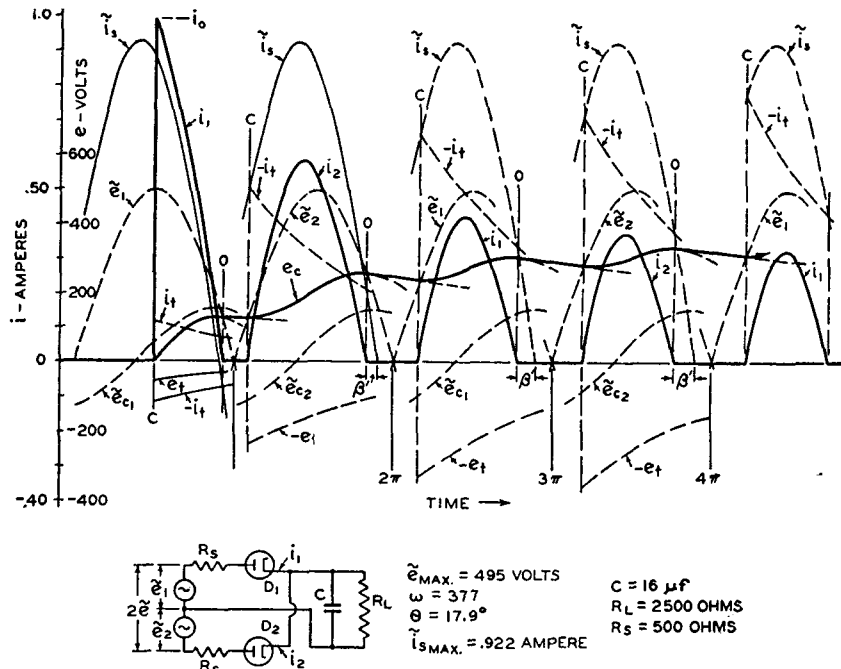


Fig. 13—Starting conditions in a full-wave, condenser-input circuit with large series resistance.

70 cycles to allow time for the discharge of condenser C_L . This cycle repeats continuously. The diode D_S in series with the tube under test protects it against damage in case it breaks down or arcs, because the diode takes up the inverse voltage if a given small reversed current determined by R_1 is exceeded. This condition is indicated by a small glow tube in shunt with D_S .

2. Coating Characteristics

A theory of electron movement and conditions in oxide coatings has been formulated after careful analysis of saturation characteristics

observed on the curve tracer. As saturated coatings produce closed reactive loops in the characteristic, it is found necessary to assume the existence of a capacitance in the diode itself. Because of its large value (see Fig. 14(c)), this capacitance requires a dielectric thickness approaching crystal spacing and, hence, must be located inside the coating. It is beyond the scope of this paper to report the many investigations which led to this particular conception.

The oxide coating is an insulator at room temperature. At increased temperatures, it becomes conductive (normal operating temperatures are between 1000 and 1100 degrees Kelvin). Electronic conduction may be thought of as occurring by relay movement of electrons under the influence of electrostatic potentials in the coating, which is a layer containing insulating oxide crystals (shaded areas in Fig. 11) interposed with metal atoms and ions (circles). These have been produced during the activation and aging processes by high cathode temperature and electrolysis. The required potential gradients can be produced by rather small potentials because of the minute distances in the structure; the potential drop throughout the coating, therefore, is low under normal conditions.

The conduction is high, when a sufficient number of relay paths not broken by oxides have been formed and when electron movement is facilitated by the loosening of the atomic structure which takes place at increased temperatures.

The coating is not necessarily a homogeneous conductor as it may consist of many sections operating in parallel but having different conductance values with individual temperature parameters. At increased plate potentials, poorly conducting sections tend to saturate, the section potential becoming more positive towards the surface. Negative-grid action of neighboring sections with higher conductivity may tend to limit emission from the surface over the poor section but the increased positive gradient towards the saturating section causes it to

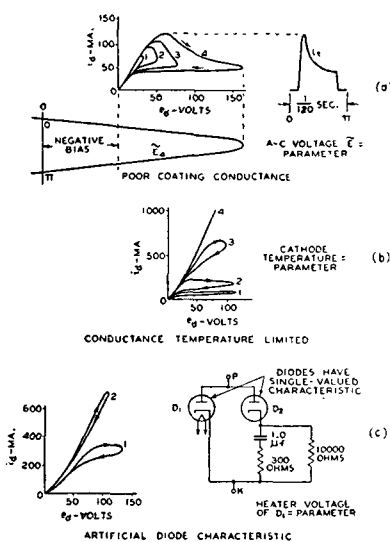


Fig. 14—Double-valued characteristics of actual and artificial diodes showing coating saturation.

draw electrons from the surrounding coating towards its surface. Further increase in current demand may then saturate the better conducting paths and may even fuse them, thus forcing current through poorer sections. Forced electron flow results in local power dissipation and temperature increases and may cause ionization and electrolysis accompanied by liberation of gas (oxygen) and formation of barium metal; i.e., it causes an accelerated activation process.

These conditions in the diode coating, therefore, should furnish a voltage-current characteristic of purely ohmic character as long as activation-gas liberation is substantially absent. Characteristics of this type are single valued. Single-valued characteristics indicate, however, unsaturated ohmic coating conductance and limiting surface

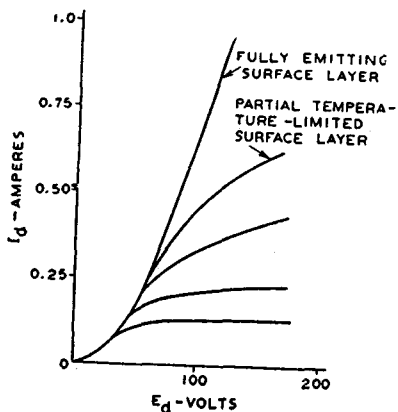


Fig. 15—Single-valued diode characteristics.

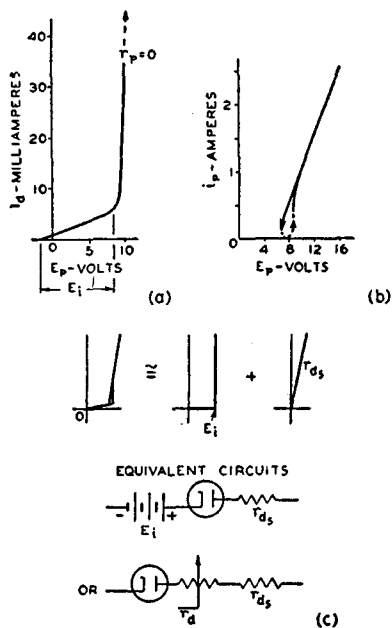


Fig. 16—Characteristics and equivalent circuit for hot-cathode, mercury-vapor diodes.

emission when moderate-current densities are involved as will be apparent from the following discussion. As cathode and coating temperatures are relatively slowly varying parameters, characteristics such as shown in Fig. 15 are observed on the cathode-ray curve tracer. The characteristic of diodes containing larger amounts of gas exhibits a discontinuity or "gas loop" (compare Fig. 16(b)) which is recognized by the fact that corresponding current values after ionization require less diode potential than before "breakdown." The characteristic, hence, is steeper than normal.

3. Transient Emission

Let us now consider the action of insulating oxides in the coating. They block many possible electron paths to sections of the surface layer which, therefore, cannot emit steady electron currents. However, electrons can be moved to the oxide surfaces and a displacement current can flow in these coating sections allowing transient-emission currents to be drawn from the corresponding surface sections.

The displacement current in the coating and the corresponding transient surface emission represent a certain fraction of the total diode current, which may permit a total emission current of short duration much in excess of the possible steady-state conduction current. The "transient-emission" current depends on the effective capacitance value of the blocking oxides, their series and shunt conductance in the coating, the emission and area of corresponding surface elements

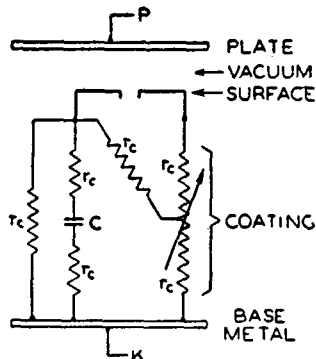


Fig. 17—Circuit network representing the coating impedance in high-vacuum diodes.

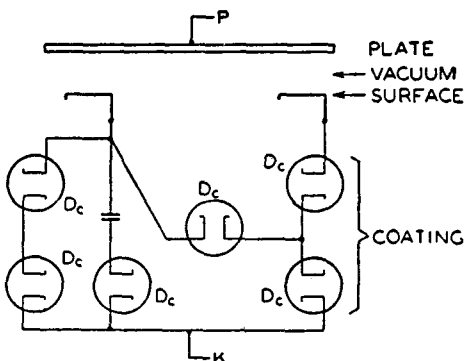


Fig. 18—Same as Fig. 17 with resistances replaced by special diodes.

to the plate as well as on the external plate-circuit impedance, and the wave form of the applied plate voltage.

For the purpose of analysis, therefore, we may draw representative networks such as shown in Figs. 17 or 18 and show the temperature-controlled coating conductances r_c as a network of "close-spaced diodes" which may conduct in two directions, each one having a single-valued characteristic which may be unsaturated or saturated depending on the assumed conditions in the coating; the conductance values of these "diodes" depend on the number of parallel or series paths they represent.

The diode contains, therefore, in its coating, a type of condenser-input load circuit, which is analyzed later on in this paper; its action explains double-valued voltage-current characteristics obtainable from the diode alone.

Consider a high plate voltage suddenly applied by means of a switch to a diode as in the circuit of Fig. 19. If the coating is not limiting, the current obtained is that at a point P on the corresponding diode characteristic. Hence, the current wave form in the circuit is as shown in Fig. 19(a). If the surface emission is assumed to be unchanged, but the coating conductance is limited, due to an insufficient number of "coating diodes" and too many nonconducting oxide groups, the wave form of Fig. 19(b) is obtained. At the instant when the switch is closed the current value i is demanded by E_d from the surface layer; the conduction current in the coating is limited to the value I_c by saturation of the "coating diodes." Because of the oxide capacitance, a displacement current can flow and charge up the oxides, but their charge may be limited by hypothetical series diodes.

The coating resistance is extremely low⁷ below saturation, but becomes infinite when the conduction current is saturated; the charging current must then flow in the plate circuit (external) of the diode.

The total plate current is, therefore, the sum of the conduction current I_c and a "transient-emission" current. The "coating transient" decays to zero the same as normal transients at a rate depending on the actual shunt-conductance value and the total series resistance in

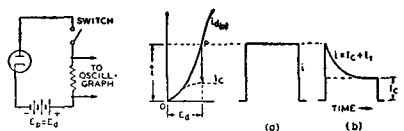


Fig. 19—Circuit for observation of peak emission transients.

the circuit (Fig. 19(b)). The decay can be changed by adding external resistance in the plate circuit. When the surface emission is good, i.e., as long as the total vacuum-space plate current is space-charge-limited, the current will rise initially to the value (point P) determined by the applied potential, but will then decay to the saturation value determined by the coating conductance.

The condition of oxide-coated cathodes can, therefore, not be judged alone by their capability of furnishing high peak currents, but the time of current flow and the current wave form must also be carefully considered, because the diode characteristic may not be single-valued. Fig. 14 shows characteristics which are not single-valued. It should be noted that the characteristic loops are formed in the opposite sense as gas loops. Their extent depends on the time interval involved and the current value exceeding the unsaturated conductance current. An artificially produced characteristic of this type is also shown in Fig. 14(c). The loop size can be varied by adjusting the cathode temperature of the shunting diode. Both diodes had single-valued characteristics.

⁷ Its magnitude depends on the number of series diodes and, hence on the barium content and thickness of the coating.

4. Current Overload and Sputter

The degree of activation is not stable during the life of the cathode. Coating conductance and surface emission change. Factors affecting the change are the coating substances, the evaporation rate of barium which depends on the base material, and the operating conditions to which the cathode is subjected. This life history of the cathode is the basis on which current ratings are established. Rectifier tubes especially are subject to severe operating conditions. If a diode is operated with too high a current in a rectifier circuit and its surface emission is decreased to the saturation value, then the tube-voltage drop will increase rapidly and cause excessive plate dissipation and destruction of the tube. Should the coating conductance in this diode decrease to a value which limits the demanded current, power is dissipated in the now-saturated coating with the result that the coating-voltage drop and coating temperature are raised. The voltage and temperature rise in the coating may cause reactivation but also may become cumulative and melt the coating material. We may consider that good conducting paths are fused or that a dielectric breakdown of oxide capacitance occurs; in any event vapor or gas discharges result from saturated coatings. In most cases breakdown occurs during one of the following inverse voltage cycles as observed on the curve tracer. A saturation loop is first formed as shown in Fig. 14 and a certain time must be allowed for diffusion of the gas into the vacuum space. Fusion of coating material may also occur during the conduction period. These breakdowns are known as "sputter," and in usual circuits destroy the cathode.

A second type of sputter is caused by the intense electrostatic field to which projecting "high spots" on the plate or cathode are subjected. The resulting current concentration causes these spots to vaporize with the result that an arc may be started. Hundreds of scintillating small spots can be observed at first at very high applied surge potentials, but may be cleared after a relatively short time.

Transient peak currents of 25 amperes per square centimeter have been observed from well-activated oxide-coated cathodes. The stable peak emission over an extended period is usually less than one-third of this value.

5. Hot-Cathode Mercury-Vapor Diodes

The breakdown voltage E_i of mercury vapor for cumulative ionization is a function of the gas pressure and temperature. It is approximately 10 volts in the RCA-83 and similar tubes. A small electron current begins to flow at $E_p = 0$ (see Fig. 16), and causes ionization

of the mercury vapor. This action decreases the variational diode resistance r_p to a very low value. The ionization becomes cumulative at a certain current value ($r_p = 0$ at 40 milliamperes in Fig. 16(a)), and causes a discontinuity in the characteristic. Hence, it is not single-valued within a certain voltage range. Beyond this range (see Fig. 16(b)), the slope (r_p) of the characteristic becomes again positive until saturation of the emitter is reached.

For circuit analysis, the mercury-vapor diode may be replaced by a bucking battery having the voltage E_i and a fixed resistance as shown in Fig. 16(c); or the diode characteristic may be replaced by an ideal rectangular characteristic and its equivalent resistance values and the series resistance r_{ds} as shown.

The first representation is adequate for most practical calculations. The value r_{ds} is in the order of 4 ohms for small rectifier tubes. The low series resistance and the small constant-voltage drop E_i are distinct advantages for choke-input filters, as they cause very good regulation; the low resistance, however, will give rise to enormously high starting transients in condenser-input circuits, in case all other series resistances are also small. The destruction of the coating in mercury-vapor diodes is caused by concentration of current to small sections of the coating surface and not by heat dissipation in the coating. Mercury-vapor diodes as well as high-perveance (close-spaced), high-vacuum diodes having oxide cathodes should, therefore, be protected against transient-current overloads when they are started in low-resistance circuits to prevent destruction of the cathode coating.

6. Protective Resistance Values

Very high instantaneous peak currents may occur in noninductive condenser-input circuits when the circuit is opened long enough to discharge the condenser, but reclosed before the cathode temperature of the diode has decreased substantially. The maximum peak current I_{max} occurs when closing the circuit at peak line voltage. At the instant of switching, C is a short circuit and the current I_{max} is limited only by the series resistance (including diode) of the circuit,

$$I_{max} = \frac{E_{max}}{R_s}.$$

For a given maximum diode current I_{dmax} and the corresponding diode peak voltage E_{dmax} , the minimum effective series resistance R_s in the circuit must hence be

$$R_s = \frac{\tilde{e}_{\max} - \hat{E}_{d\max}}{\hat{I}_{d\max}}.$$

This limiting resistance must be inserted in series with low-impedance sources (power line in transformerless sets). Commercial power transformers for radio receivers have often sufficient resistance besides some leakage reactance to limit starting currents to safe values.

III. CIRCUIT ANALYSIS

General

The rectifier diode is a switch operated in synchronism with the applied alternating-current frequency. Switching in reactive circuits causes transients. The total current in the circuit may be regarded as the sum of all steady-state currents and transient currents within the time between two switching operations. Steady-state voltages (e_s) and currents (i_s) in the particular circuit before and after switching are determined without difficulty. It is very helpful to draw them approximately to scale and with proper phase relation.

The switching time of the diode is then located on the graph. Currents change at switching time t_0 from i_1 to $i_2 = i_{s(2)} + i_t$ and voltages from e_1 to $e_2 = e_{s(2)} + e_t$. The transients i_t or e_t are zero, when the current change does not occur in an inductive circuit or when a voltage change is not required on a capacitance at the time of switching. A sudden change Δi_L or Δe_c demanded at t_0 causes transients. They initially cancel the change Δi_L or Δe_c because an inductance offers infinite impedance to an instantaneous change in total current and a capacitance offers zero impedance to an instantaneous voltage change.

The initial transient values are, therefore,

$$i_{t(0)} \text{ in } L = -\Delta i_L$$

and

$$e_{t(0)} \text{ on } C = -\Delta e_c.$$

The transients decay exponentially from their initial value.

According to the decay time of the transients, fundamental rectifier circuits may be classified into two principal groups: (1) circuits with repeating transients in which the energy stored in reactive elements decreases to zero between conduction periods of the diode; and (2) circuits with chain transients in which (a) the magnetic energy stored in the inductance of the circuit remains above zero value, and (b) the electric energy stored in the capacitance of the circuit remains

above zero value. The much used "choke-input" and "condenser-input" circuits fall under the second group.

We shall analyze the operation in important circuits, i.e., the full-wave choke-input circuit and condenser-input circuits.

1. The Full-Wave Choke-Input Circuit

a) Operation of circuits with L and R_s in the common branch circuit

Circuit and operation are shown in Fig. 20. The analysis is made by considering first one of the diodes short-circuited to obtain the phase

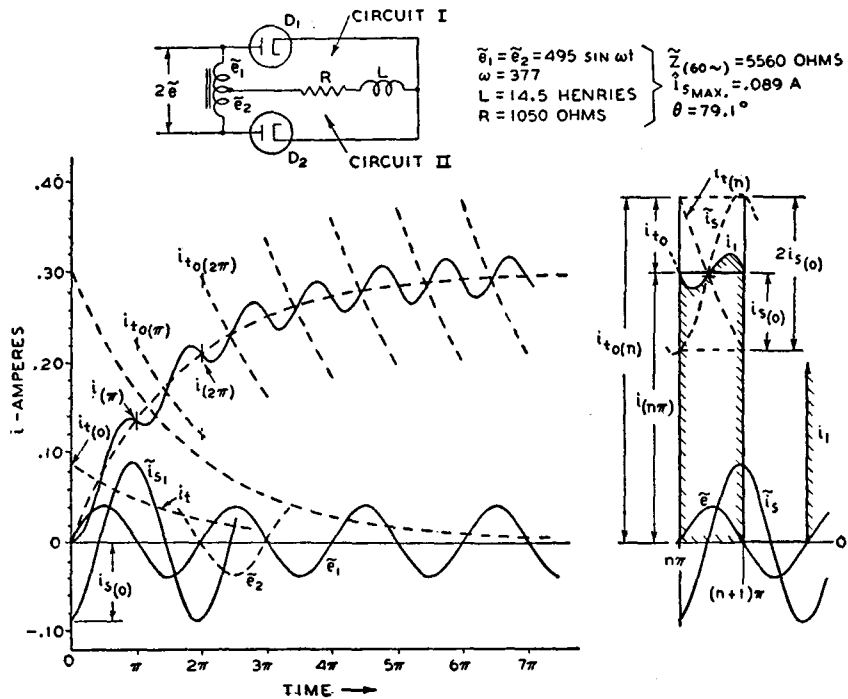


Fig. 20—Starting and operating conditions of an aperiodic full-wave, choke-input rectifier circuit.

relation of the alternating voltage \tilde{e} , and the steady-state current \tilde{i}_s , as shown. If we assume that the diode D_1 closes the circuit I at the time $\tilde{e} = 0$, a transient i_t with the initial value $i_{t(0)} = -\tilde{i}_{s(0)}$ will flow in the circuit. The total current i is the sum of the currents $\tilde{i}_{s1} + i_t$. It starts, therefore, at zero and rises as shown until the second switching operation occurs at the commutation time $t = \pi$ when the second diode D_2 receives a positive plate voltage. The total current i in circuit II after $t = \pi$ is again the sum of currents $\tilde{i}_{s2} + i_t$ (\tilde{i}_{s2} has reversed polarity with respect to \tilde{i}_{s1} and is not shown in Fig. 20) but

the initial value $i_{t(0)}$ of the second transient is increased by the value $i_{(\pi)}$ now flowing in the common circuit inductance L .

The current $i_{t(0)}$ increases, therefore, at every new switching time until the decay of the transient $i_{t(n)}$, during the time $t = \pi$, is numerically equal to the steady-state current rise $2\tilde{i}_{s(0)}$. For the final operating current at the n th commutation time (see right side of Fig. 20)

$$(i_{(n\pi)} - \tilde{i}_{s(0)}) (1 - e^{-Rs/2FL}) = -2\tilde{i}_{s(0)}$$

$$i_{(n\pi)} = \tilde{i}_{s(0)} - (2\tilde{i}_{s(0)}/1 - e^{-Rs/2FL}). \quad (7)$$

A broken line is shown connecting all commutation-current values. This line represents closely the average current \bar{I} in the common circuit branch. The final average current \bar{I} in the load resistance R_s is given by (7), when the transient decay $i_{t(n)}$ during the time π (Fig. 20) can be regarded as linear (low steady-state power factor of circuit). The average plate current per diode is $\bar{I}_p = 0.5\bar{I}$, since each diode conducts alternately, and passes a current pulse shown by the shaded area in Fig. 20. With the numerical values of the circuit Fig. 20 substituted in (7) we obtain

$$i_{(n\pi)} \cong \bar{I} = 0.298 \text{ ampere.}$$

The oscillogram in Fig. 21 was taken on circuit Fig. 20.

- b) The full-wave choke input circuit with capacitance-shunted resistance load

For large capacitance values the by-passed load resistance R_L of practical circuits is equivalent to a battery having a voltage $\bar{E}_B = \bar{I}R_L$, where \bar{I} is the average load current or battery-charging current. The circuit operation (see Fig. 22) is described by obtaining \bar{I} as a function of \bar{E}_B . The final commutation current $i_{(n\pi)}$ which is closely the average current \bar{I} is given by

$$\bar{I} \cong i_{(n\pi)} = (I_B + \tilde{i}_{s(0)}) - 2\tilde{i}_{s(0)}/(1 - e^{Rs/2FL}) \quad (7b)$$

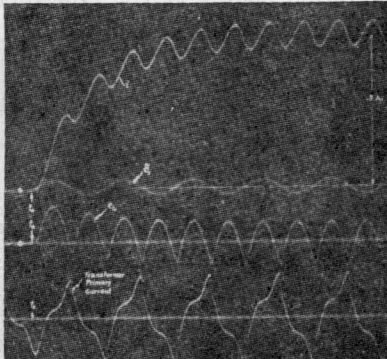


Fig. 21—Oscillograms taken with circuit of Fig. 20.

and similar to (7) except for an increase of the transient term due to the battery current $I_B = \bar{E}_B/R_s$.

Equation (7b) is valid only over a range of load or battery voltage (\bar{E}_B) in which switching time and conduction period of the diodes are constant ($\phi = \pi$). This range is shown by the solid part of curve F in Fig. 22 and ends at a particular current and voltage of the circuit characteristic marked the "critical point."

The critical point is the operating condition at which the instantaneous current i in the common branch circuit has zero value at one instant. An analysis shows that in the range $\bar{E}_B = \bar{e}_{\max}$ to $\bar{E}_B = E_B'$ each diode circuit operates independently as a half-wave rectifier circuit (battery-charger operation, curve H in Fig. 22). Current commutation begins at E_B' ; the diode circuits begin to interact, but the conduction angle is still $\phi < \pi$.

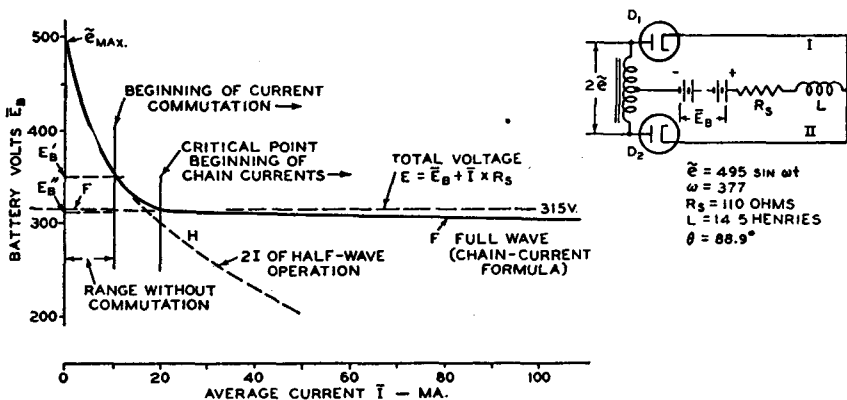


Fig. 22—Operating characteristic of a full-wave, choke-input rectifier circuit with battery load \bar{E}_B or resistance load $R_L = \bar{E}_B/I$ shunted by a large capacitance.

The conduction angle increases from $\phi = 0$ at $\bar{E}_B = \bar{e}_{\max}$ to $\phi = \pi$ at the critical point E_B'' which marks the beginning of chain current operation.

The critical operating condition is obtained by solving for $i = 0$ with $\phi = \pi$ or by equating the direct current to the negative peak value of the total alternating current in L . The critical point is hence specified by a certain current or by a certain ratio K of direct-current resistance to alternating-current impedance in the circuit. With reference to the equivalent circuit treated in the following section, a relation to the fundamental alternating-current component of the rectified current (see (10)), i.e., to the impedance $Z_{(2F)}$, at double line frequency is more useful. We set, therefore,

$$\frac{(R_s + R_L)}{Z_{(2F)}} = K \quad (8)$$

and determine significant values of K for particular circuit impedance conditions.

If we neglect harmonics higher than $2F$, which contribute little to the peak value because of phase shift and increasing attenuation in L , the peak ripple current (equation (10)) becomes

$$i_{\min} = 4/3\pi (\tilde{e}_{\max}/Z_{(2F)})$$

and setting it equal to the average current

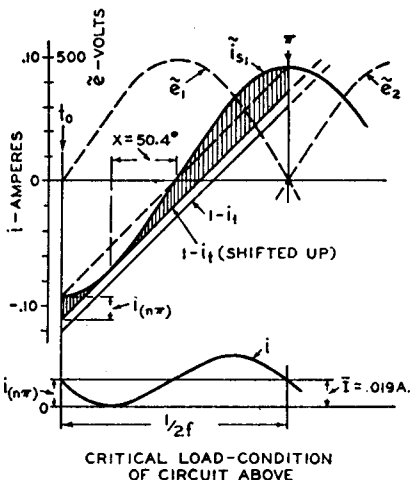
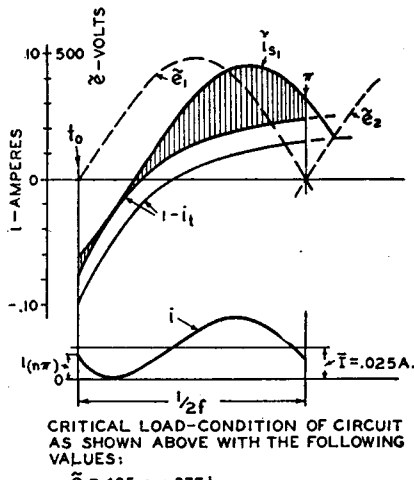


Fig. 23—Graphic solution for the critical load condition with negligible series resistance.



CRITICAL LOAD-CONDITION OF CIRCUIT AS SHOWN ABOVE WITH THE FOLLOWING VALUES:

$$\begin{aligned} \tilde{e} &= 495 \sin 377t \\ R_s &= 3770 \text{ OHMS} \\ L &= 10 \text{ HENRIES}, \omega L = 3770 \text{ OHMS} \\ \theta &= 45^\circ \end{aligned}$$

Fig. 24—Same as Fig. 23 but with large series resistance.

$$I = 2/\pi (\tilde{e}_{\max}/(R_s + R_L))$$

we obtain $K = 1.5$ for the ratio as shown in (8).

The exact solution for the critical current can be obtained from a graphic analysis by simple reasoning for the case $R_s = 0$. The general solution will only be indicated. It is obtained by drawing the complementary curve $(1 - i_t)$ of the total transient beginning at the time $\tilde{e} = 0$ (see Figs. 23 and 24) and shifting it upward until it touches the current i_s , thus solving for $i = 0$ at the point of contact. Note that $i_{(n\pi)}$ is the same at t_0 and π in both cases shown.

For $R_s = 0$, the transient section becomes a straight line having the slope $2/\pi$ and running parallel to the peak-to-peak connecting line of \tilde{i}_s . The sine-wave slope $2/\pi = -\cos x$ gives the point of contact at $X = 50.4$ degrees (Fig. 23), and the peak ripple current is obtained from

$$i_{\min} = \tilde{i}_{s\max} \left(\sin 50.4^\circ - \frac{50.4}{90} \right) = 0.211 \tilde{i}_{s\max}$$

$$= 0.211 \frac{\tilde{e}_{\max}}{\omega L}.$$

Equating this value to the average current given by (10), we obtain the value $K = 1/0.211 = 1.51$ for circuits with $R_s = 0$. The graphic analysis of circuits with larger resistance (see Fig. 24) furnishes K values sufficiently close to 1.5 to justify the use of this constant for all practical purposes. For practical circuits with $2\omega L \gg 1/2\omega C$ we may further write $Z_{(2F)} \cong 2\omega L$ and obtain the *critical inductance*⁸

$$L_0 \cong (R_s + R_L)/2\omega K = (R_s + R_L)/6\pi F. \quad (9)$$

- c) Equivalent circuit for the chain current operating range ($\phi = \pi$ or $(R_s + R_L) < 1.5Z_{(2F)}$)

Inspection of (7b) shows that average and commutation current are directly proportional to the sum of the battery current \bar{I}_B and a term having a constant current value " I_K " for a given circuit and constant line voltage. Equation (7b) can be changed into the form

$$\bar{I} = (I_K R_s) / (R_L + R_s),$$

indicating that the secondary circuit may be replaced by an equivalent circuit without switches and energized by a voltage which contains a constant direct-current component $\bar{E} = I_K R_s$. The equivalent voltage in the circuit is the commutated sine wave resulting from the sequence of positive half cycles $+\tilde{e}_1$ and $+\tilde{e}_2$ in the range $\phi = \pi$. The equivalent circuit is shown in Fig. 25(a). The single generator may be replaced by a battery and a series of sine-wave generators (Fig. 25(b)) having amplitudes and frequencies as given by the following equation of the

⁸ The relation $L_0 = R_L/1000$ was given on an empirical basis for $\omega = 377$ by F. S. Dellenbaugh, Jr., and R. S. Quinby, "The important first choke in high-voltage rectifier circuits," *QST*, vol. 16; pp. 14-19; February, 1932.

commutated sine wave:

$$e = \frac{2\tilde{e}_{\max}}{\pi} \left(1 - \frac{2 \cos 2F}{1 \cdot 3} - \frac{2 \cos 4F}{3 \cdot 5} - \frac{2 \cos 6F}{5 \cdot 7} - \dots \right). \quad (10)$$

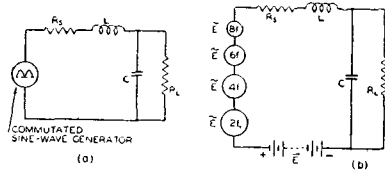
All current components in the circuit may now be computed separately by steady-state methods; the direct-current component is the total average voltage \bar{E} in the circuit.

Some useful relations of voltage components are: Line voltage induced in one half of the secondary winding (root-mean-square)

$$|\tilde{E}| = 1.1\bar{E}$$

Total average voltage

$$\bar{E} = \begin{cases} 0.90 |\tilde{E}| \\ 0.637\tilde{e}_{\max} \end{cases}$$



Voltage of frequency $2F$ (root-mean-square)

$$|\tilde{E}|_{2F} = \begin{cases} 0.424 |\tilde{E}| \\ 0.471\bar{E} \end{cases} \quad (11)$$

Fig. 25—Components of equivalent and practical full-wave, choke-input circuits.

Voltage of frequency $4F$ (root-mean-square)

$$|\tilde{E}|_{4F} = \begin{cases} 0.085 |\tilde{E}| \\ 0.0945\bar{E} \end{cases}$$

Total choke voltage (root-mean-square)

$$|\tilde{E}|_L = \begin{cases} \sqrt{|\tilde{E}|^2 - \bar{E}^2} \\ 0.482\bar{E} \end{cases}$$

The current components in the common circuit branch are calculated from the above voltages divided by the impedance of one branch circuit at the particular frequency. Because the current is commutated every half cycle of the line frequency from one to the other branch circuit, the average current in each diode circuit is one half of the total

average current; and root-mean-square values of currents or current components in each branch circuit are obtained by multiplying the root-mean-square current values in the common circuit branch by $1/\sqrt{2}$. The peak current in each diode circuit has the same value as in the common circuit branch.

Average load current

$$I = \frac{E}{R_s + R_L}$$

Average plate current (per diode)

$$I_p = 0.5I \quad (12a)$$

Double-frequency current (root-mean-square) in common circuit branch

$$|I|_{2F} = \frac{|E|_{2F}}{Z_{(2F)}}$$

Total current (root-mean-square) in common circuit branch

$$|I|_L = \sqrt{I^2 + |I|_{2F}^2}$$

Root-mean-square diode current or root-mean-square current per transformer winding

$$|I|_p = \frac{|I|_L}{\sqrt{2}} \quad (12b)$$

Peak diode current

$$i_d = I + (|I|_{2F} \times \sqrt{2})$$

The total power dissipated in diode and load circuits of the practical secondary circuit shown in Fig. 25(c) is the sum of the power losses in the circuit resistances. In equation form, it is

Total power = series-resistance loss

+ choke-core loss

+ direct-current power in load.

The plate dissipation per diode is given by

$$P_d = 0.5 |I| L^2 \times |r_d|. \quad (13)$$

With reference to (5), we have

$$P_d = 0.5 |I| L^2 \times \frac{\bar{e}_d}{I} \quad (14)$$

where \bar{e}_d is the diode voltage taken from the static diode characteristic at the output-current value I .

d) Regulation

The regulation of choke-input circuits is determined by the total series resistance R_s , since the voltage \bar{E} in the circuit is constant in the useful chain current range for an energizing alternating voltage of constant value. Thus, the regulation curve has the slope R_s (see Fig. 26), which includes the diode resistance. The regulation curve

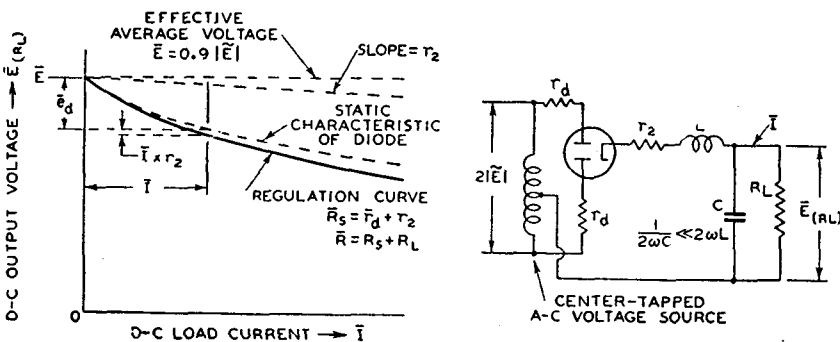


Fig. 26—Regulation characteristic of a full-wave, choke-circuit with high-vacuum diode.

for a circuit with high-vacuum diodes is the sum of the 3/2-power-law diode characteristic and the ohmic series resistance r_2 of one branch circuit as shown in Fig. 26. The curve is correct for constant voltage \bar{e} and beyond the critical current value. In practical circuits, the voltage source \bar{e} has a certain equivalent resistance, which must be added to r_2 . The regulation curve Fig. 26 is invalid below the critical current value and must be replaced by a curve following the laws discussed for Fig. 22.

The equivalent internal resistance of the rectifier circuit as a direct-current supply source is the slope of the regulation curve at the current value under consideration. This value should be used for steady-output conditions only, since the reactances in the load circuit cause transients at the instant of sudden load changes.

2. The Condenser-Input Circuit

In rectifier circuits with shunt-condenser-input loads, the condenser is alternately charged and discharged. In the final state of operation, charge and discharge are balanced. The graphic analysis of such circuits is comparatively simple and readily followed. Formulas for the calculation of specific circuit conditions are easily derived from the constructions.

a) Circuits without series resistance

The graphic analysis of a half-wave rectifier circuit without series resistance (R_s) is illustrated in Fig. 27. Steady-state voltage \tilde{e} and

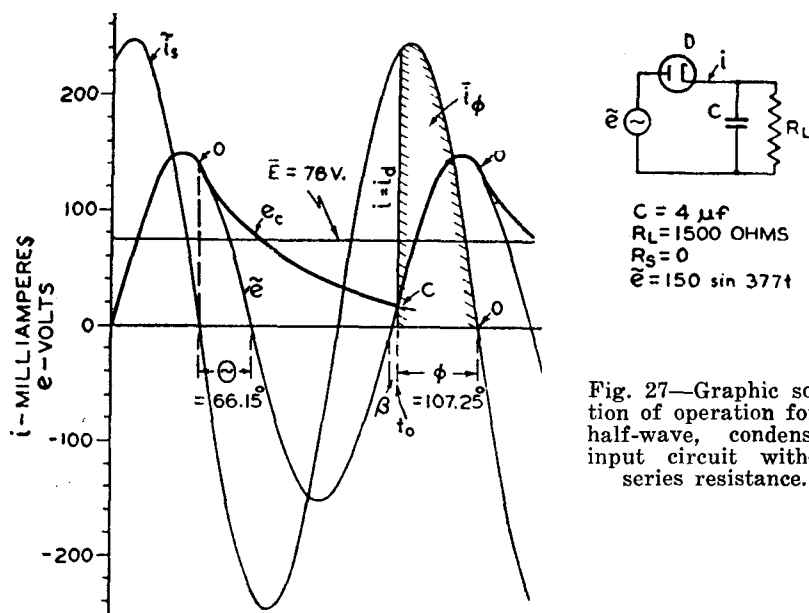


Fig. 27—Graphic solution of operation for a half-wave, condenser-input circuit without series resistance.

current i_s are constructed on the assumption that the diode is short-circuited. The steady-state condenser voltage \tilde{e}_c coincides with \tilde{e} because $R_s = 0$.

The diode timing is as follows:

The diode opens the circuit at point 0 when the diode current becomes zero.

Since the condenser-discharge circuit consists of C and R_L , the condenser voltage decays exponentially as shown. At point C it has become equal to the energizing voltage \tilde{e} . The diode becomes conducting and closes the circuit. Because there is no potential difference between the steady-state voltages \tilde{e} and \tilde{e}_c , the condenser does not

receive a transient charge. The current, therefore, rises instantly to the steady-state value of the \tilde{i}_s curve and follows it until zero at point 0.

The timing of the full-wave circuit in Fig. 28 is quite similar. The time for the condenser discharge through R_L is reduced since e_o meets the positive half cycle \tilde{e}_2 and thus closes the circuit through D_2 . Point C in Fig. 28 is located at a higher value of \tilde{e} than in Fig. 27. The conduction angle ϕ is consequently reduced although C , R_L , and Θ have the same values in both circuits. The average current in the full-wave circuit is, therefore, smaller than twice that of the half-wave circuit.

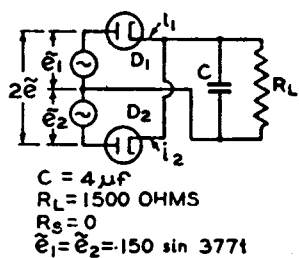
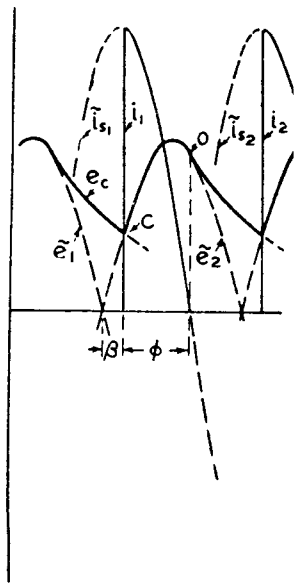


Fig. 28—Graphic solution of operation for a full-wave, condenser-input circuit without series resistance.



Some of the relations obtainable directly from Figs. 27 and 28 are

i. the conduction angle $\phi = 180^\circ - \Theta - \beta$. (15)

The intersection of \tilde{e} with the decaying voltage e_t furnishes for half-wave operation ($n = 1$) and full-wave operation ($n = 2$)

ii. $\sin \beta = \sin \Theta e^{-(\pi + \Theta + \beta)/\omega C R_L}$ for $n = 1$ }
 and $\sin \beta = \sin \Theta e^{-(\Theta + \beta)/\omega C R_L}$ for $n = 2$ } (16)

where π , Θ , and β in the exponents are in radius. This equation may be solved graphically or by trial and error, varying β .

iii. The average current during conduction time is

$$I_{(\phi)} = I_s (1 - \cos \phi) / \phi.$$

It is the area under a sine-wave section divided by its base. Hence, the average plate current is as shown in (iv).

iv. $I_p = \bar{i}_{(\phi)} \frac{\phi}{2\pi} = \frac{i_s}{2\pi} (1 - \cos \phi).$ (17)

v. Average current I and voltage \bar{E} in the load resistor are

$$\left. \begin{array}{l} I = I_p \quad \text{for } n = 1 \\ I = 2I_p \quad \text{for } n = 2 \\ \bar{E} = IR_L \end{array} \right\}. \quad (18)$$

vi. The diode peak current i_p is, obviously

$$\left. \begin{array}{l} i_p = \bar{i}_s \quad \text{for } \phi > 90^\circ \\ i_p = \bar{i}_s \sin \phi \quad \text{for } \phi < 90^\circ \end{array} \right\}. \quad (19)$$

and

The performance of these circuits, hence, is determined by their power factor ωCR_L and the phase number n . It will be evident from the following that the series resistance R_s of practical circuits appears as an additional parameter which cannot be neglected.

b) Circuits with series resistance

In circuits with series resistance, the steady-state condenser voltage \bar{e}_c does not coincide with the supply voltage \bar{e} , as illustrated in Figs. 29 and 30. Phase displacement and magnitudes of current and voltage under steady-state conditions are required for analysis of the circuit and are computed in the conventional manner. The parallel circuit $C \parallel R_L$ is converted into an equivalent series circuit to determine the angles Θ and Θ' by which \bar{i}_s is leading \bar{e}_c and \bar{e} , respectively. The steady-state condenser voltage \bar{e}_c in the parallel circuit equals the voltage across the equivalent circuit as shown by the vector diagram in Fig. 30.

The diode opens the circuit at the instant $i_d = 0$. For circuit constants as in Fig. 30, the diode current i_d substantially equals \bar{i}_s at the time of circuit interruption because the transient component i_t' of the current, as shown later, has decayed to a negligible value. Point 0

is thus easily located. In circuits with large series resistance, however, $i_d = 0$ does not coincide with $\tilde{i}_s = 0$ due to slow decay of the transient i'_t . In both cases the condenser voltage $e_{c(0)}$ equals the voltage $\tilde{e}_{(0)}$ at the time 0, because $i_d = 0$ and consequently there is no potential difference on R_s and transients do not occur at 0. The condenser voltage decays exponentially on R_L from its initial value at 0, as discussed for circuits with $R_s = 0$, and meets the supply voltage \tilde{e} again at point C. At this instant (t_0), the diode closes the circuit. Current and voltage, however, do not rise to their steady-state values as in

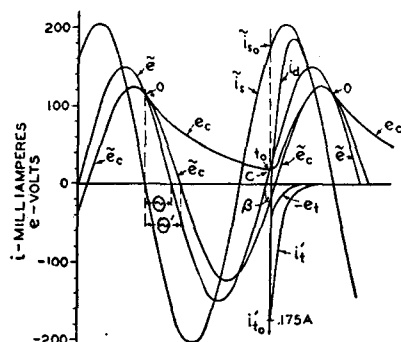
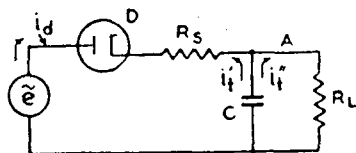
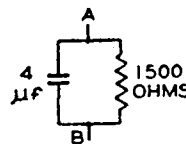


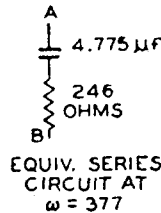
Fig. 29 (above)—Graphic solution of operation for a half-wave, condenser-input circuit with series resistance.



$$R_s = 220 \text{ OHMS} \quad \tilde{e}_{\text{MAX}} = 150 \text{ V.} \\ R_L = 1500 \text{ OHMS} \quad \omega = 377 \\ C = 4 \mu\text{F}$$

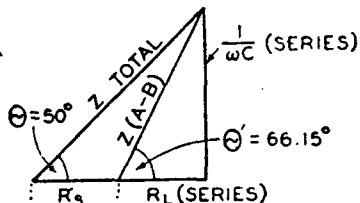


PARALLEL LOAD CIRCUIT



EQUIV. SERIES CIRCUIT AT $\omega = 377$

Fig. 30 (right)—Equivalent series circuit for the analysis of half-wave, condenser-input circuits with $R_s > 0$.



circuits with $R_s = 0$, because the steady-state voltage $\tilde{e}_{c(0)}$ differs from the line voltage $\tilde{e}_{(0)}$ by the amount $\Delta e_c = \tilde{i}_{s(0)} R_s$. A transient voltage of initial value $e_{t(0)} = -(\tilde{i}_{s(0)} R_s)$ occurs on C. It drives transient currents i'_t and i''_t determined by Ohm's law through the resistances R_s and R_L respectively. (See Fig. 30).

The transients e_t and i_t' prevent voltage and current from following the steady-state wave forms, as

$$i_d = \tilde{i}_s + i_t' = \tilde{i}_s - \tilde{i}_{s(0)} e^{-t/(R_s || R_L)C} \quad (20)$$

and

$$e_c = \tilde{e}_c + e_t = \tilde{e}_c + R_s \tilde{i}_{s(0)} e^{-t/(R_s || R_L) C} \quad (21)$$

between the time t_0 and the opening time at 0.

For small values R_s and C , the transient decay is rapid as shown in Fig. 29 and point 0 is readily determined. The oscillogram Fig. 31 was taken on the circuit Fig. 30 and checks the graphic construction.

The solution of operating conditions in circuits with large time constants requires additional steps, as e_c and i_d do not reach steady-state values before $\tilde{i}_s = 0$. The diode opens the circuit earlier at an angle β' , which increases from cycle to cycle as shown for a full-wave

circuit in Fig. 13. The condenser voltage e_c rises in successive conduction periods until its numerical decay over R_L equals the numerical rise during ϕ . This final condition is shown in Fig. 32(b). The graphic solution for the final operating condition is illustrated in Fig. 32(a) and is made as follows:

Steady-state current \tilde{i}_s and voltage \tilde{e}_s are drawn with proper phase relation. A closing time t_0 is assumed near the estimated average output voltage, condition A in Fig. 32(a) assumes $\tilde{i}_{s(0)} = 0.7A$ and $\tilde{e}_{(0)} = 258$ volts at t_0 . The current transient i_t' is subtracted graphically from \tilde{i}_s . Only two points t_1 and

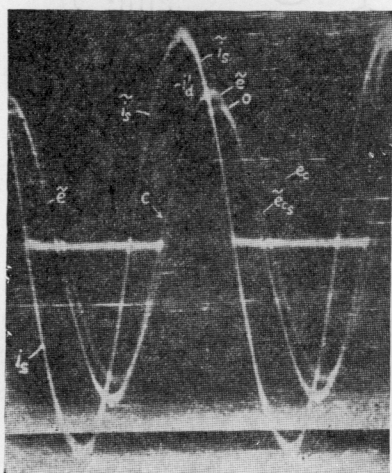


Fig. 31—Oscillograms taken with circuit of Fig. 30.

t_2 are necessary near the intersection; t_1 gives a decay of 57.4 per cent and then t_2 gives a decay of 50 per cent from $\tilde{i}_{s(0)}$. The intersection with the \tilde{i}_{s1} curve gives a solution for i_p equal to 0 and determines line 0, which gives $\tilde{e}_1 = 308$ volts which is also the voltage e_c . This voltage decays now over R_L until it intersects the following half cycle \tilde{e}_2 for closing time C_2 at point A = 283 volts which is the second closing time. As this voltage is higher than the initially assumed voltage ($\tilde{e}_{(0)} = 258$ volts), the final condition is not yet reached. A second trial marked B was made with an initial voltage $\tilde{e}_{s(0)} = 333$ volts and furnished $\tilde{e}_{(2)} = 319$ volts at C_2 . The correct condition $\tilde{e}_{(0)} = \tilde{e}_{(2)}$ is obtained from the auxiliary graph in Fig. 32(a) in which the voltage pairs A and B are connected by a straight line, which intersects the 45-degree lines $\tilde{e}_{(0)}C_1 = \tilde{e}_{(0)}C_2$ at the point X, and provides the solu-

tion for the final condition $\bar{e}_{(0)} = 306$ volts. If desired this value can be checked and corrected by exact calculation.

The final construction in Fig. 32(b) was made with this value. The shaded areas include the amplitude values i_d and e_c during ϕ which are given by (20) and (21).

The average current during ϕ is the area under the sine-wave section minus the area under the exponential curve i_t , both divided by the base. This furnishes

$$\begin{aligned} i_{d(\phi)} &= i_{s\max} [(\cos \beta' - \cos (\phi + \beta')) \\ &\quad - \omega CR' (1 - e^{-\phi/\omega CR'}) \sin (\Theta + \beta)]/\phi \end{aligned} \quad (22)$$

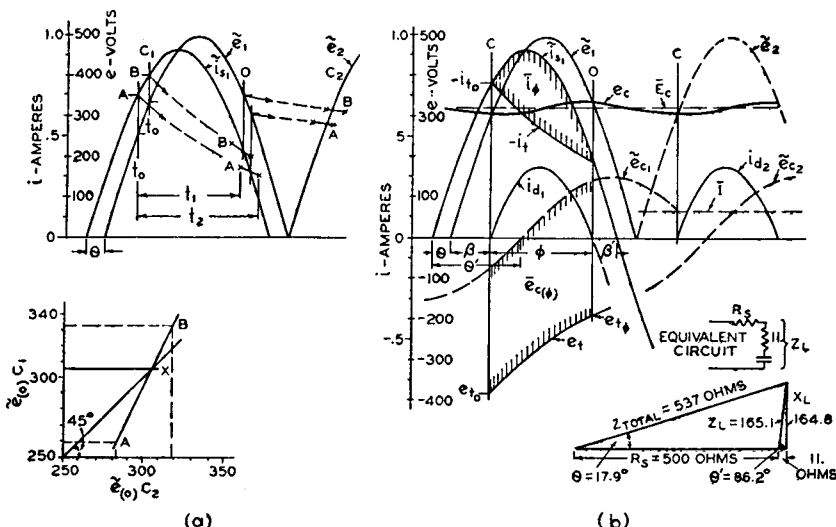


Fig. 32—Graphic solution of final operating conditions for circuit in Fig. 13.

with $R' = R_s || R_L$ and ϕ , β and β' determined graphically from the construction or by trial of values. The average plate current per diode is again

$$I_p = i_{d(\phi)} \phi^\circ / 360^\circ$$

and the direct load current in this full-wave circuit is $I = 2I_p$. In case of large time constants, as in the example, the average condenser voltage \bar{e}_c is quite accurately obtained from

$$\bar{e}_c = 0.5 (e_{c(0)} + e_{c(\phi)}) \quad (23)$$

and the load current by Ohm's law $I = \bar{E}_o / R_L$.

The root-mean-square values of ripple voltage and diode current are needed for many calculations. They may be obtained for all cases from

$$|E|_{(\text{ripple})} = 0.321 (e_{c(\text{max})} - e_{c(\text{min})}) \quad (24)$$

and

$$|I_s| = 1.1 I_s \sqrt{\frac{360^\circ}{\phi}}. \quad (25)$$

Equation (24) holds within 10 percent for wave shapes varying from a sine-wave to a saw-tooth and (25) gives better than 5 per cent accuracy for all wave shapes occurring in condenser-input circuits.

c) Generalized operation characteristic (steady-state operation)

It has been shown that the conduction angle is a function of the circuit constants in condenser-input circuits. The section of the energizing voltage \bar{e} utilized during conduction time has, therefore, no fixed value as in choke-input circuits where $\phi = 180$ degrees and where the voltage \bar{e} during ϕ is a half sine wave. It is, therefore, not possible to derive a general equivalent circuit for condenser-input circuits which contains a voltage source of fixed wave shape and magnitude.⁹

Steady-state conditions as well as transients are controlled by the circuit constants, which are contained in the product ωCR_L . The angle ϕ depends further on the relative magnitudes of R_L and R_s and is, therefore, described in general if also the ratio R_s/R_L is known. General curve families may thus be evaluated which show the dependent variables \bar{E} , i , and I in terms of ratio versus the independent variable ωCR_L for various parameter values R_s/R_L . The series resistance R_s includes the equivalent diode resistance which is evaluated by means of (6), because the current wave is periodic in the final operating state. The reasoning leading to (6) is not applicable to a single transient, as obtained for starting conditions of rectifier circuits.

Generalized characteristics have been evaluated for the three types of circuits shown in Fig. 9. The characteristics in Figs. 3, 4, and 5 show the average voltage \bar{E} across the load resistance R_L as a function of ωCR_L and R_s for half-wave, full-wave, and voltage-doubling circuits. They permit the solution of the reversed problem to determine the magnitude of the applied voltage necessary to give a certain

⁹ The equivalent voltage may be expressed by a Fourier series for each individual case as shown for the simplest case $R_s = 0$ by M. B. Stout in footnote reference 1; the method, however, is hardly suitable for practical circuit analysis.

average voltage output for a given load. The series-resistance value \bar{R}_s includes the equivalent average resistance \bar{r}_d of one diode and the power-transformer resistances as reflected into one secondary winding. As their complete calculation required too much time, the characteristics were plotted from accurately measured values. The measurements were made on circuits of negligible inductive reactance. Series-resistance values in these circuits were determined accurately by the method shown in Fig. 10. Table II gives a number of calculated values which show the accuracy of the curves to be approximately 5 per cent or better.

Table II

Type of Condenser- Input Circuit	$n\omega CR_L$	$\frac{\bar{R}_s}{n R_L}$	θ degrees	ϕ degrees	$\frac{\bar{E}}{\bar{e}_{\max}}$	$\frac{i_d}{I_s}$	$\frac{ I_p }{I_s}$
Half-Wave $n = 1$	0.5	0	26.5	153.5	0.335	3.33	1.69
	1.	0	45.0	134.0	0.384	3.68	1.81
	2.	0	63.4	111.6	0.486	4.61	2.00
	2.26	0	66.15	106.4	0.503	4.91	2.02
	4.	0	75.9	87.1	0.623	6.60	2.24
	8.	0	82.9	65.1	0.742	9.86	2.60
	16.	0	86.4	48.6	0.862	13.92	3.00
	32.	0	88.2	35.3	0.930	19.90	3.51
	64.	0	89.1	25.1	0.996	27.5?	4.16
	2.	0.10	—	121.	0.434	4.48	1.9
	2.26	0.147	50.	123.	0.428	4.42	1.88
	4.	0.05	65.1	99.3	0.632	5.28	2.1
	4.	0.10	56.	108.4	0.537	5.14	2.0
Full-Wave $n = 2$	1.	0	26.5	142.5	0.644	3.47	1.75
	2.	0	45.0	121.0	0.678	4.17	1.90
	4.	0	63.4	92.6	0.740	6.06	2.17
	4.52	0	66.15	86.8	0.744	6.55	2.24
	8.	0	75.9	67.0	0.816	9.30	2.55
	16.	0	83.0	49.0	0.885	13.74	3.00
	32.	0	86.4	35.6	0.945	19.70	3.50
	64.	0	88.2	25.4	0.999	27.1?	4.15
	4.	0.05	—	104.	0.671	5.43	2.05
	4.52	0.0735	50.	105.	0.636	5.35	2.04
	8.	0.05	56.	90.	0.710	6.20	2.20
	30.2	0.10	17.9	100.6	0.646	5.39	2.08

In compiling the data for the current-ratio characteristics in Fig. 6, it was found that the three rectifier-circuit types could be shown by a single family after a "charge factor" n was added to the product of the circuit constants ωCR_L and to R_s as shown in Table II.

The factor n is unity for the half-wave circuit. For the full-wave circuit, n is 2 because the condenser C is charged twice during one cycle. For the voltage-doubling circuit, n is $\frac{1}{2}$ because the two condensers require together twice the charge to deliver the same average current at double voltage. The values in the table indicate that the factor n is actually not a constant. The mean value of the current ratios does, however, not depart more than 5 per cent from the true value, the error being a maximum in the steep portion of the curves and decreasing to zero at both ends. The upper section of Fig. 6 shows the ratio of root-mean-square current to average current per diode plate. This family is of special interest in the design of power transformers and for computation of diode plate dissipation.

Fig. 7 shows the root-mean-square value of the ripple voltage across R_L in per cent of the average voltage.

The voltage-doubling circuit shown with the other two condenser-input circuits in Fig. 9 may be regarded in principle as a series connection of two half-wave rectifier circuits. Each condenser is charged separately during conduction time of one diode, but is discharged in series with the other condenser during the time of nonconduction of its associated diode. The analysis of operation is made according to the method discussed but will not be treated. The average anode characteristics of RCA rectifiers are shown in Fig. 8. The method of carrying out a practical analysis by use of these curve families has been outlined in the first section of this paper.

APPENDIX

System of Symbols

The number of special symbols and multiple indexing have been greatly reduced by introducing four special signs for use with any symbol.

- 1) The symbols in general are of standard notation, lower case letters i , r , indicate instantaneous, sectional, or variable values and capital letters I and R indicate steady values.
- 2) Special values
 - a) *Sinusoidal voltages or currents* are indicated by a sine-wave sign above the symbol \bar{e} , \bar{i} , \bar{E} . Their maximum values are indicated by index, \bar{e}_{\max} , \bar{E}_{\max} .
 - b) *Peak values* are indicated by circumflex; \hat{e}_c , \hat{i} , \hat{r}_d , maximum peak values are written \hat{i}_{\max} , etc.
 - c) *Average values* are indicated by a horizontal bar; \bar{E} , \bar{I} , \bar{R} .

- d) Root-mean-square values are indicated by vertical bars $|E|$, $|I|$, $|R_s|$.
- 3) An index in parenthesis specifies the time at which the symbol is valid, i.e., its numerical value. Hence, $\bar{i}_{s(\pi)}$ is the steady-state alternating-current value at the time π and $i_{t(0)}$ is the transient current at the time 0. When used with an average or root-mean-square value, the time index specifies the period over which average or root-mean-square values are taken, such as $\bar{I}_{(\phi)}$, $|i_p|_{(\phi)}$. A conduction time index (ϕ) on resistance values such as \bar{r}_d , \bar{R}_s is unnecessary. (See definition.)

SPACE-CURRENT FLOW IN VACUUM-TUBE STRUCTURES*†

By

B. J. THOMPSON

RCA Laboratories,
Princeton, N. J.

Summary—From well-known formulas for space-current in diodes and for amplification factor in triodes, interelectrode capacitance, plate current, and potential distribution in triodes and multi-grid tubes are determined through use of the concept of planes of equivalent potential. By the same means, amplification factor in multigrid tubes is derived.

INTRODUCTION

VACUUM-TUBE design is a subject which has intrigued many workers, largely, one may suspect, because it has presented many possibilities for ingenious methods of analysis. The resulting knowledge of the design factors which determine the various performance characteristics of tubes is quite complete and is expressed in terms which can readily be applied to practical tube-design problems. In spite of this state of the art, the general tendency is to make use of the more "scientific" phases of tube design to aid qualitative understanding rather than to supply specific design information. In this paper, the writer presents some of the concepts of vacuum-tube analysis which he has found informative and useful.

First, space-current flow in diodes will be discussed. Then, methods will be presented for reducing triodes and multigrid tubes to equivalent diodes. Amplification factor, interelectrode capacitance (cold), and electron transit time will be covered. The writer claims little originality and no novelty in this material. Some effort has been made to give credit to the proper sources.

A. DIODE THEORY

Ideal Case

The simplest vacuum tube is the diode. The behavior of multi-electrode tubes may be described most readily in terms of the behavior of a diode. For these reasons our treatment will start with the diode.

In the ideal diode, electrons are emitted from the cathode in un-

* Decimal Classification: R131.

† Reprinted from *Proc. I.R.E.*, September, 1943.

limited numbers at zero velocity and a part of these are drawn over to the anode under the influence of the positive field established by its potential.

In Figure 1, K represents the infinite plane cathode at zero potential and A the plane anode at a positive potential E_b , spaced a distance d_{kp} from the cathode. Let us suppose first that no electrons are emitted from the cathode. The potential distribution will then be as represented by the line a , the gradient at all points being E_b/d_{kp} . If now the cathode begins to emit a limited supply of electrons, all of these electrons will be drawn to the anode. The electrons move at a finite velocity and, therefore, there is a certain number of them in the space at all times. The field set up by the negative "space charge" of these electrons acts to depress the potential in the space below that of the first condition, increasing the field near the anode and decreasing it near the cathode. This condition is shown by line b .

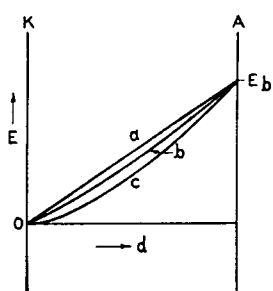


Fig. 1—Potential distribution in a diode with varying amounts of space charge.

If the rate of emission of electrons is continually increased, all of the emitted electrons will be drawn to the anode and the gradient at the cathode continually reduced until the gradient reaches zero. Since the electrons are assumed to be emitted with zero velocity, they can not move against a retarding field; therefore, there will be no increase in anode current with further increase in emission beyond this point. The condition of zero gradient at the cathode is represented by the line c in Figure 1.

The mathematical analysis of the ideal parallel-plane case is quite simple. It will be presented here as an example of this type of analysis. Poisson's equation in rectangular co-ordinates is

$$\frac{\partial^2 E}{\partial x^2} + \frac{\partial^2 E}{\partial y^2} + \frac{\partial^2 E}{\partial z^2} = -4\pi\rho. \quad (1)$$

Since there is no gradient in directions parallel to the cathode and anode, the equation becomes simply

$$\frac{\partial^2 E}{\partial x^2} = -4\pi\rho. \quad (2)$$

We may also write that

$$I = \rho v \quad (3)$$

and

$$v = (2eE/m)^{1/2} \quad (4)$$

where ρ is the space-charge density, E the potential at any point a distance x from the cathode, v the velocity of the electrons at x , I the current per unit area, and e and m the charge and mass of the electron.

On combining the last three equations, we obtain

$$\frac{d^2E}{dx^2} = -4\pi \frac{I}{(2eE/m)^{1/2}}. \quad (5)$$

If we multiply both sides by dE/dx and integrate once, we obtain

$$\frac{1}{2} \left(\frac{dE}{dx} \right)^2 = \frac{8\pi I}{(2e/m)^{1/2}} E^{1/2} + F_0^2 \quad (6)$$

where F_0 is the field at the cathode. If we let F_0 equal zero, a second integration gives us

$$E^{3/4} \left| \begin{array}{c} E_b \\ 0 \end{array} \right. = 3(\pi I)^{1/2} \left(\frac{m}{2e} \right)^{1/4} x \left| \begin{array}{c} d_{kp} \\ 0 \end{array} \right. \quad (7)$$

$$\text{or} \quad I = \frac{1}{9\pi} \left(\frac{2e}{m} \right)^{1/2} \frac{E_b^{3/2}}{d_{kp}^2} \\ = 2.33 \times 10^{-6} (E_b^{3/2}/d_{kp}^2). \quad (8)$$

This is the well-known Langmuir-Child¹ equation for space-charge-limited current flow per unit area between parallel-plane electrodes. It means that for each square centimeter of cathode or anode area 2.33 microamperes of current will flow with 1 volt difference in potential and a distance of 1 centimeter between cathode and anode, and that a current of 233 microamperes per square centimeter will flow if the potential be raised to a little over 30 volts or the distance reduced to 1 millimeter.

The foregoing analysis is for parallel-plane electrodes. The case of concentric cylinders, of much practical interest, is very much less simple to analyze and, therefore, only the result will be presented here. Excellent analyses are available in the literature².

¹ I. Langmuir and K. T. Compton, "Electrical discharges in gases—Part II," *Rev. Mod. Phys.*, Vol. 3, pp. 238-239; April, 1931.

² See pp. 245-249 of footnote reference 1.

The current in amperes per centimeter length of the concentric cylinders is given by the well-known Langmuir equation

$$I = 14.66 \times 10^{-6} (E_b^{3/2}/r_b \beta_b^2) \quad (9)$$

where r_b is the radius of the anode and β_b^2 is a function depending on the ratio of anode radius to cathode radius. Tables and curves of β have been published³. It will be noted that the current again depends on the 3/2 power of the anode voltage; otherwise, the expressions at first glance do not appear very similar. Part of this difference is due to the fact that one expression is for current per unit area, while the other expression is for current per unit length.

It will be interesting to put the two expressions in similar form. Let us divide equation (9) by $2\pi r_b$. Equation (9) then becomes identical with equation (8) except for the presence of the term β_b^2 in the denominator and the fact that the distance r_b is measured from the axis of the cylindrical system. When the ratio of anode diameter to cathode diameter becomes very large, β_b^2 approaches unity and, of course, the distance between cathode and anode approaches r_b as a limit. At this limit, then equations (8) and (9) become identical, and we observe the interesting fact that the anode current flow per unit area is the same in a cylindrical system with fine-wire filament as it would be in a parallel-plane system with the same distance between cathode and anode. This statement, of course, neglects the effect of initial velocity of emission.

At the other limit where the cathode and anode diameters approach each other the system is obviously essentially a parallel-plane one. The value of β_b^2 then changes rapidly and maintains such a value that $r_b^2 \beta_b^2$ is equal to d_{kp}^2 .

The fact that the two expressions give identical results at the two limits of ratio of anode-to-cathode diameter should not lead one to suppose that the expressions are approximately identical for intermediate ratios. Where the anode diameter is from 4 to 20 times the cathode diameter, the current calculated from (8) is in excess of that indicated by (9) by very nearly 20 per cent. This is the maximum error that would result from the use of expression (8) for cylindrical structures.

The potential distribution between cathode and anode may be calculated most usefully from the expressions for current. From (8) we may write

³ See pp. 247-248 of footnote reference 1.

$$E_b^{3/2}/d_{kp}^2 = E^{3/2}/x^2$$

or

$$E = E_b (x/d_{kp})^{4/3}.$$

In other words, the potential between parallel planes varies as the four-thirds power of the distance from the cathode in the case of space-charge-limited currents.

The potential distribution between concentric cylinders is less simple. We may write from (9)

$$E_b^{3/2}/r_b\beta_b^2 = E^{3/2}/r\beta^2$$

or

$$E = E_b (r\beta^2/r_b\beta_b^2)^{2/3}$$

where β^2 is taken for the ratio r/r_k . This expression is not analytical, the values of β and β_b being obtained from curves or tables.

Effects of Velocities of Emission

Electrons are emitted from a heated surface with a random distribution of velocities in all directions. The velocities which concern us in the present analysis are those normal to the surface of the cathode. This velocity distribution may be expressed most simply as follows: $n/n_0 = e^{-Ee/kT}$ where n is the number of electrons out of the total number n_0 which has a sufficient velocity to reach a plane electrode parallel to the cathode at a negative potential of E , T is the temperature of the cathode, and k is Boltzmann's constant. Expressed in terms of current this becomes $I = I_s e^{-Ee/kT}$ where I is the current reaching the negative electrode and I_s is the total emission current from the cathode. To carry this out experimentally, it is necessary that the collector electrode be placed so close to the cathode that space-charge effects do not cause a potential minimum in space.

We initially assumed that all electrons were emitted with zero velocity and that, therefore, the field at the cathode would not be negative. In the practical case where all electrons have finite velocities normal to the cathode, all of the emitted electrons must reach a positive anode parallel to the cathode unless at some point between cathode and anode a negative potential exists.

Fig. 2 shows the potential distribution between parallel-plane cathode and anode for successively higher values of emission. Line *a* represents the case where there is no emission, and, therefore, no space charge, with resulting constant potential gradient between cathode and anode. Line *b* shows the case where there is sufficient

emission to reduce the gradient at the cathode just to zero. This is similar to the condition represented by *c* in Fig. 1 with the important difference that now all electrons pass over to the anode because of their finite velocities of emission.

Any further increase in cathode emission, however, will cause the potential near the cathode to become slightly negative as shown in line *c*. In this case all electrons having velocities less than E_m are turned back to the cathode, while those electrons having greater velocities of emission pass on to the anode. Further increases in cathode emission cause the potential minimum to become more negative with the result that a larger fraction of the emitted electrons return to the cathode. For continued increase in cathode emission, however, there will always be some slight increase in anode current.

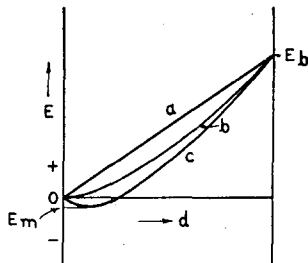


Fig. 2.—Potential distribution in a diode, showing the effect of initial velocity of electron emission.

The results obtained from the simple analysis based on zero velocity of emission are obviously not applicable to this practical case if precision is desired. Since a greater maximum potential difference ($E_b + E_m$) is acting over a shorter effective distance ($d_{kp} - d_{km}$) and since the average velocity of electrons is higher because of their initial velocities and hence the space-charge effect of the electrons is less, it is obvious that the space-charge-

limited current flow for a given anode potential is greater in the actual case than in the ideal.

Langmuir⁴ has presented a complete analysis of the space-charge-limited current flow with initial velocities of emission. He has shown that a good approximation may be made by the use of (8) with a correction for the reduced effective distance and the increased effective potential. His equation is as follows:

$$I_b = 2.33 \times 10^{-6} \frac{(E_b - E_m)^{3/2}}{(d_{kp} - d_{km})^2} \times \left[1 + \frac{0.0247T^{1/2}}{(E_b - E_m)^{1/2}} \right] \quad (10)$$

where T is the cathode temperature in degrees Kelvin. I_b is in amperes per unit area. E_m is negative in sense. The value of d_{km} in centimeters may be calculated from the approximate expression

⁴ See pp. 239-244 of footnote reference 1.

$$d_{km} \approx 0.0156 (1/1000I_b)^{1/2} (T/1000)^{8/4}$$

The value of E_m is given by

$$E_m = - (T/5040) \log_{10} (I_s/I_b)$$

More complete results of Langmuir's analysis are too cumbersome to be presented here. The use of (10) should lead to errors not greatly in excess of 2 per cent even under extreme conditions.

It is interesting to observe from Langmuir's calculation in a practical case where the cathode temperature is 1000 degrees Kelvin, the emission density greatly in excess of the anode current, and the anode current density 1 milliampere per square centimeter, that the distance from cathode to virtual cathode is approximately 0.016 centimeter (0.006 inch). Thus, in modern close-spaced vacuum tubes the position of the virtual cathode cannot be neglected.

The error involved in using (9) as compared with the exact solution for cylindrical structures is less than in the corresponding case of parallel planes. For a discussion of the effect of initial velocities in this case, the reader is referred to Langmuir and Compton⁵.

The potential distribution between parallel planes, taking into account initial velocities, may best be determined by the use of a plot presented by Langmuir and Compton⁶.

B. TRIODE THEORY

Triode Mu Formulas

The earliest analysis of the electric field existing between parallel planes with a parallel-wire screen interposed is that of Maxwell⁷. In this it is assumed that the spacings between the planes and the screen are large compared with the spacings between wires and that these in turn are large compared with the wire diameter. The result expressed in vacuum-tube terminology is

$$\mu = - \frac{2\pi d_{sp}}{a \log_e (2 \sin \pi r/a)}$$

$$\text{or } \mu = \frac{2\pi d_{sp}}{a \log_e (a/2\pi r)} \quad (\text{where } \pi r/a \text{ is small}).$$

⁵ See pp. 252-255 of footnote reference 1.

⁶ See Fig. 42, p. 243 of footnote reference 1.

⁷ J. C. Maxwell, "Electricity and Magnetism," third edition, 1904, Vol. 1, section 203.

In these expressions, d_{gp} is the distance from the center of the grid wires to the plate, a the spacing between grid wires ($a = 1/n$, where n is the number of wires per unit length), and r is the radius of the grid wires. It will be noted that the distance between grid and cathode does not appear.

This formula is in serious error when the spacing between grid wires is not large compared with the wire diameter, as is frequently the case. Because of this, van der Bijl developed empirically the formula $\mu = Cd_{gp} r n^2 + 1$, where C is equal to 160 for parallel planes. An obvious defect of this expression is that μ can never be less than unity.

The most generally useful and accurate formula for amplification constant which has been published is that developed by Vogdes and Elder⁸. This analysis assumes that the spacing between grid wires is small compared with the distances between the grid and the other electrodes. The development is as follows.

Fig. 3 represents the geometry of the vacuum tube. By means of a conformal transformation, this same geometry may be represented in different co-ordinates. In such a transformation, equipotential surfaces and flux lines still cross at right angles and all laws of electricity still apply.

Suppose the geometry represented in the w plane in Fig. 3 be transformed to the z plane by the transformation $z = e^{2\pi nw}$.

Since

$$z = x + jy$$

and

$$w = u + jv$$

then

$$x + jy = e^{2\pi nu} \times e^{j2\pi nv} = \rho e^{j\theta}.$$

This transformation is represented in Fig. 4. The cathode is a point at the origin. The grid wires become a single figure intersecting the x axis as $e^{-2\pi nr}$ and $e^{2\pi nr}$. The center of the grid wires is at $x = 1$. The anode is a circle about the origin of radius equal to $e^{2\pi nd_{gp}}$.

The figure representing the grid wires is not a circle. If r is less than $a/2\pi$, however, it can be shown readily that the figure is essentially circular and it will be assumed, therefore, that such is the case. If the figure is a circle, its radius is

$$\frac{e^{2\pi nr} - e^{-2\pi nr}}{2} = \sinh 2\pi nr$$

⁸ B. F. Vogdes and F. R. Elder, "Formulas for the amplification constant for three-element tubes," *Phys. Rev.*, Vol. 24, p. 683; December, 1924.

and its center is located at

$$x = \frac{e^{2\pi nr} + e^{-2\pi nr}}{2} = \cosh 2\pi nr.$$

In Fig. 3, if the anode were removed to infinity and a potential applied to the grid, the successive equipotential surfaces at greater distances from the grid would become more and more nearly planes until, at distances several times a , the surface could be regarded as essentially a plane. Therefore, under the limitations of our assumptions concerning relative spacings, the anode plane may be considered to be the equipotential surface due to the field of the grid alone. This

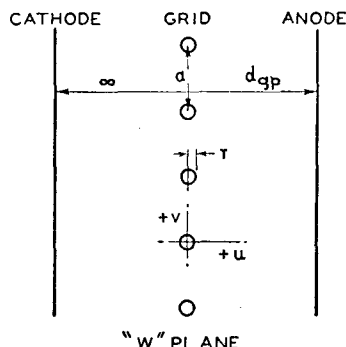


Fig. 3—Cross section of a triode in normal co-ordinates.

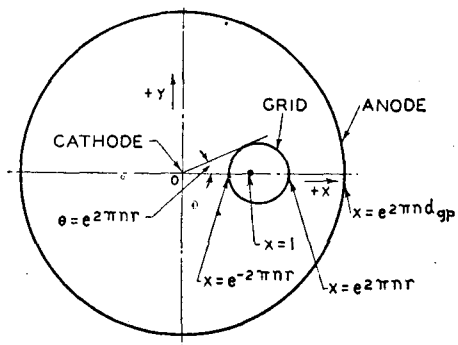


Fig. 4—Cross section of the triode of Fig. 3 transformed from the w plane to the z plane.

is equivalent to saying that a circle of radius $e^{2\pi nd_{gp}} - \cosh 2\pi nr$ drawn about the "center" of the grid wire in Fig. 4 does not differ materially from a circle of radius $e^{2\pi nd_{gp}}$ drawn about the origin. The justification for this assumption may be checked by considering the rather extreme case where $nd_{gp} = 0.50$ and $nr = 0.03$. Then $e^{2\pi nd_{gp}}$ equals 23.1 and $\cosh 2\pi nr$ equals 1.02.

The convenient result of these assumptions is that a line charge placed at the "center" of the circular grid wire, Fig. 4, produces equipotential surfaces at the surface of the grid wires and at the anode, since the charge on the cathode located at minus infinity must be zero.

Let us place a charge $-Q$ at the "center" of the grid wire. The potentials E_k , E_g , and E_a of the cathode, grid, and anode become

$$E_k = C + 2Q \log \cosh 2\pi nr$$

$$E_g = C + 2Q \log \sinh 2\pi nr$$

$$E_a = C + 2Q 2\pi n d_{gp}.$$

If the cathode potential be taken as zero,

$$\begin{aligned} E_g &= 2Q \log \sinh 2\pi nr - 2Q \log \cosh 2\pi nr \\ &= 2Q \log \tanh 2\pi nr \end{aligned}$$

and $E_a = 2Q 2\pi n d_{gp} - 2Q \log \cosh 2\pi nr$.

Under these circumstances, the amplification constant may be defined as $\mu = -E_a/E_g$,

$$\text{whence } \mu = \frac{\log \cosh 2\pi nr - 2\pi n d_{gp}}{\log \tanh 2\pi nr}.$$

The assumptions made in this derivation invalidate the expression for use with relatively very close spacings between electrodes. The same type of analysis as that presented by Vogdes and Elder may be made to give more rigorous results. Salzberg⁹ has carried out such an analysis. It differs from that just presented chiefly in that an additional line charge is placed on the x axis, Fig. 4, outside the anode at such a position as to make the true anode cylinder an equipotential surface. Therefore, the anode may be allowed to approach much more closely to the grid. This leads to an expression accurate for cases where the spacing between the anode and grid is small compared with the wire spacing, though not when the wire spacing is small compared with the wire diameter. Salzberg's expression is

$$\mu = \frac{\log \cosh 2\pi nr - 2\pi n d_{gp}}{\log \tanh 2\pi nr - \log (1 - e^{-4\pi n d_{gp}} \times \cosh^2 2\pi nr)}.$$

There is no obviously useful definition of amplification factor in the purely electrostatic case (no space charge) when the charge density induced on the cathode is not uniform. It is possible by extension of the analysis described above, however, to arrive at an expression for the charge distribution on the cathode when the spacing between cathode and grid is finite. Salzberg has carried out such an analysis¹⁰. It departs from that of the cathode at infinity by considering the poten-

⁹ Bernard Salzberg, "Formulas for the amplification factor of triodes," Proc. I.R.E., Vol. 30, pp. 134-138; March, 1942.

¹⁰ Not published.

tials in space produced by a line charge at the cathode in addition to the others.

The amplification-factor formulas here given may be applied to cylindrical tubes if $r_g \log(r_a/r_g)$ is substituted for d_{gp} , where r_g and r_a are the radii of the grid and anode, provided r/r_g is small.

Equivalent Potentials in Triodes

For most practical purposes in calculating the electric fields at cathode, anode, and the space between, except very near the grid, a potential may be assigned to the plane of the grid. In other words, it is assumed that an equipotential plane may be substituted for the grid without altering the electric fields. This would be true only when the grid wires are small and closely spaced in comparison with the spacings between grid and cathode and anode.

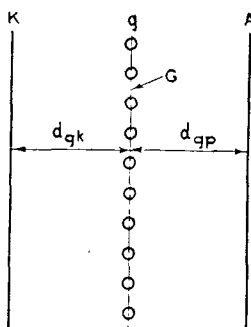


Fig. 5—Triode with equivalent plane G at grid.

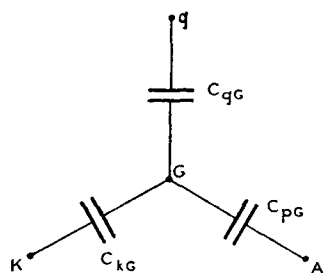


Fig. 6—Star network of the capacitances of the triode of Fig. 5.

The equivalent potential of the plane of the grid E_g may be derived in several ways. The most simple with which the writer is familiar is the following. The capacitance between anode and the equivalent plane G at the grid, Fig. 5, is $C_{pG} = 1/4\pi d_{gp}$ and the capacitance from cathode to G , $C_{kg} = 1/4\pi d_{kg}$ while, by definition $C_{gG} = \mu C_{pG}$.

In the star network of capacitances, Fig. 6,

$$E_g = \frac{E_c C_{gG} + E_b C_{pG} + E_k C_{kg}}{C_{gG} + C_{kg} + C_{pG}}.$$

Let us make E_k equal to zero. Then,

$$E_g = \frac{\mu E_c + E_b}{\mu + 1 + d_{gp}/d_{gk}}.$$

or

$$E_G = \frac{E_c + E_b/\mu}{1 + 1/\mu + d_{gp}/d_{gk}\mu}.$$

The physical basis for this analysis is that the anode can influence the field at the cathode only by acting through the grid plane. By definition, the grid has μ times the influence of the anode. It is obvious that this reasoning implicitly assumes that amplification factor is proportional to grid-anode spacing, for we might just as well have called the cathode the anode. The quantity $d_{gp}/d_{gk}\mu$ is simply the reciprocal of the amplification factor of the grid with respect to the cathode.

We shall find it convenient to determine another equivalent-potential plane. The equivalent potential of the grid plane depends on grid

and anode potentials and on grid-cathode and grid-anode spacings. Is there an equivalent plane the potential of which depends only on grid and anode potentials and grid-anode spacing?

In Fig. 7, E_G is the equivalent potential of the grid. If the constant potential gradient between grid and cathode extended past the grid, the potential E at any point a distance x from the grid would be

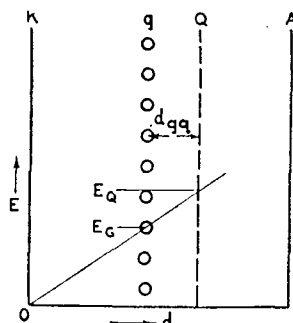


Fig. 7 — Determination of equivalent potential E_G of the Q plane.

$$E = E_G (1 + x/d_{gk})$$

$$= \frac{(E_c + E_b/\mu)}{1 + 1/\mu + d_{gp}/d_{gk}\mu} \cdot (1 + x/d_{gk}).$$

We wish to find a potential $E = E_q$ at a distance $x = d_{gq}$ from the grid which is independent of d_{gk} . At such a point the ratio

$$\frac{1 + x/d_{gk}}{1 + 1/\mu + d_{gp}/d_{gk}\mu}$$

must be independent of d_{gk} . Obviously this means that

$$\frac{x}{d_{gk}} = \frac{d_{gp}/d_{gk}\mu}{1 + 1/\mu}$$

or

$$x = d_{gp}/(\mu + 1) = d_{gq}.$$

The potential E_q is given by

$$E_q = \frac{E_c + E_b/\mu}{1 + 1/\mu}.$$

Applications of this equivalent-potential plane will be given

Interelectrode Capacitances in Triodes without Space Charge

The direct capacitance between grid and anode, C_{gp} , may be calculated readily from the expression for E_G , the equivalent potential of the plane of the grid.

The capacitance per unit area from anode to the equivalent plane of the grid is $C_{pG} = 1/4\pi d_{gp}$.

Then $C_{gp} = C_{pG} \frac{dE_G}{dE_g} = \frac{1}{4\pi d_{gp}} \left(\frac{1}{1 + 1/\mu + d_{gp}/d_{gk}\mu} \right).$

Similarly $C_{gk} = \frac{1}{4\pi d_{gk}} \left(\frac{1}{1 + 1/\mu + d_{gp}/d_{gk}\mu} \right).$

By definition $C_{pk} = \frac{C_{gk}}{\mu} = \frac{1}{4\pi d_{gk}} \left(\frac{1}{\mu + 1 + d_{gp}/d_{gk}} \right).$

These derivations are for the parallel-plane case. The case of cylindrical electrodes may be treated in a similar fashion.

Amplification Factor in Multigrid Tubes

The analysis of multigrid tubes may be readily carried out by use of the second expression for equivalent potential E_q .

In Fig. 8, the Q plane is to be substituted for g_2 and A . Its potential is

$$E_q = \frac{E_{c2} + E_b/\mu_{g2p}}{1 + 1/\mu_{g2p}}$$

and its distance from g_1 is $d_{g1p} = d_{g1g2} + d_{g2p}/(1 + \mu_{g2p})$. We now have a triode and can calculate its μ . The simplest expression is $\mu_{g1q} = (\mu'_{g1g2}/d_{g1g2}) d_{g1q}$ where μ'_{g1g2} is the amplification factor of g_1 with respect to a plane at g_2 .

Now

$$\begin{aligned}\mu_{g1g2} &= \mu_{g1q} (dE_{c2}/dE_q) \\ &= \mu_{g1q} (1 + 1/\mu_{g2p}) \\ &= \mu'_{g1g2} (d_{g1q}/d_{g1g2} (1 + 1/\mu_{g2p})).\end{aligned}$$

On substituting the expression for d_{g1q} in this equation, one may reduce it to the following form by simple manipulation: $\mu_{g1g2} = \mu'_{g1g2} + \mu'_{g1p}/\mu_{g2p}$ where μ'_{g1p} is the value μ_{g1p} would have if g_2 were removed.

Of course $\mu_{g1p} = \mu_{g1g2}\mu_{g2p}$ whence¹¹ $\mu_{g1p} = \mu'_{g1g2}\mu_{g2p} + \mu'_{g1p}$. The direct capacitance between g_1 and g_2 may also be determined readily, since $C_{g1g2} = C_{g1q} (dE_q/dE_{c2})$. Also, the capacitances between grids and anode or cathode may be determined in the same manner.

By an obvious extension of the method, amplification factors and capacitances may be determined in structures containing any number of grids.

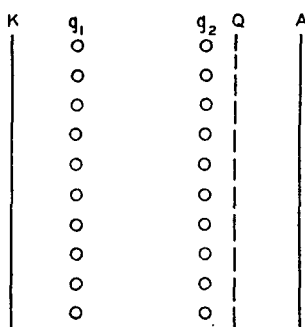


Fig. 8—Determination of amplification factor and inter-electrode capacitance in multigrid structures by use of the Q plane.

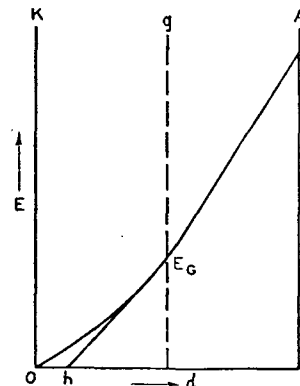


Fig. 9—Apparent location h of the cathode as seen from the grid.

Effects of Space Charge on Potential Distribution in Triodes

In the case where space charge between grid and anode may be neglected (as is usually the case in receiving tubes with negative control grids), a quite precise equivalent diode may be constructed by the use of the first expression for equivalent potential with a space-charge correction. Fig. 9 shows the potential distribution in a triode with space-charge-limited current. It is obvious that the field at the grid is the same as would exist without space charge if the cathode were at point h , determined by drawing a tangent to the potential curve at the grid. If it be assumed that the potential between cathode

¹¹ For an alternative derivation see S. Koizumi, "On the amplification constants of multi-electrode vacuum tubes," *Jour. I.E.E. (Japan)*, pp. 505, 857; 1930.

and grid varies as the four-thirds power of distance, d_{gh} is three fourths of d_{gk} . Hence, we must modify the expression for E_G as follows:¹²

$$E_G = \frac{E_c + E_b/\mu}{1 + 1/\mu + (4/3)(d_{gp}/d_{gk}\mu)}.$$

The analysis of the current-voltage relationship of a triode may be made directly from the diode case by the use of this equivalent-diode expression. If in the equivalent diode the space current $I_b = f(E_G)$ the cathode current (equal to the plate current with negative grid) is given directly. The transconductance g_m is found by taking the derivative of $f(E_G)$ with respect to E_c . The plate conductance $1/r_p$ is found by taking the derivative¹³ of $f(E_G)$ with respect to E_b .

Electron Transit Time in Negative-Grid Triodes

The electron transit time in any electrode structure may be calculated readily if the potential distribution is known. In general

$$t = \int \frac{dx}{v} = \left(\frac{m}{2e} \right)^{1/2} \int \frac{dx}{E^{1/2}}.$$

The calculation of transit time in the absence of space charge is obvious. In a parallel-plane diode with space-charge-limited current, the transit time from cathode to anode may be calculated if it be assumed that

$$E = E_b(x/d_{kp})^{4/3}$$

whence

$$t = \left(\frac{m}{2e} \right)^{1/2} \frac{d_{kp}^{2/3}}{E_b^{1/2}} \int_0^{d_{kp}} x^{-2/3} dx$$

¹² B. D. H. Tellegen, "The calculation of the emitted current in a triode," *Physica*, Vol. 5e, pp. 301-315; 1925.

¹³ Note added April 6, 1943: Fremlin¹⁴ discusses several old expressions for equivalent diode potential, none of which is similar to that given above, and then derives an expression for anode current of a triode starting from the known condition of grid and anode at such potentials as to maintain the space-potential distribution of a diode undisturbed to the anode (grid at "space potential"). Unfortunately, no simple analysis of this sort is valid when there is appreciable space charge in the grid-anode space as is implicit under Fremlin's assumptions. In the case of negligible grid-anode space charge, Tellegen's expression seems satisfactory.

¹⁴ J. H. Fremlin, "Calculations of triode constants," *Elec. Communications*, July, 1939.

$$\begin{aligned}
 &= \left(\frac{m}{2e} \right)^{1/2} \frac{3d_{kp}}{E_b^{1/2}} \\
 &= 5.05 \times 10^{-8} (d_{kp}/E_b^{1/2})
 \end{aligned}$$

where t is in seconds, d_{kp} in centimeters, and E_b in volts. In other words, the electron take three times as long to pass from cathode to anode as if it had traveled at the final velocity the entire distance, and half again as long as if it had been uniformly accelerated.

The cylindrical analysis is not so simple but may be carried out as presented by W. R. Ferris.¹⁵

In the case of electron transits between grid and anode, the integration is carried out with the initial velocity of the electron corresponding to the equivalent potential of the grid.

¹⁵ W. R. Ferris, "Input resistance of vacuum tubes as ultra-high-frequency amplifiers," *Proc. I.R.E.*, Vol. 24, pp. 82-108; January, 1936.

THE STORAGE ORTHICON AND ITS APPLICATION TO TELERAN*†

BY

S. V. FORGUE

Research Department, RCA Laboratories Division,
Princeton, N. J.

Summary

An orthicon type of pickup tube, having a very high capacity target, and operating with a low beam current, has been used successfully to pick up a radar PPI presentation for television reproduction. By virtue of its large storage capacity the tube can reproduce for hundreds or even thousands of television scans information presented but once on the PPI screen.

(18 pages, 9 figures)

* Decimal Classification: R339 \times 629.132.5 \times R583 \times R537.† *RCA Review*, December, 1947.

ELECTRON TUBE PHONOGRAPH PICKUP*†

BY

H. F. OLSON AND J. PRESTON

Research Department, RCA Laboratories Division,
Princeton, N. J.

Summary

Fundamental experimental and theoretical investigations in the field of mechanical and acoustical vibrating systems in recent years have made possible the transfer of controlled vibrations through a vacuum-tight shell. This paper describes a vacuum tube mechano-electronic transducer based on such a system. A thin rod of extremely low inertia passing through the envelope acts as the anode. Motion of the anode changes the distance between anode and cathode, thus producing a signal. Outputs as large as 2 volts can be obtained from standard records.

Pickups for both vertical and lateral recordings have been constructed.

(4 pages; 17 figures)

* Decimal Classification: R391.12.

† *Audio Eng.*, August, 1948.

PERFORMANCE OF 931-A TYPE MULTIPLIER IN A SCINTILLATION COUNTER*†

BY

G. A. MORTON AND J. A. MITCHELL

Research Department, RCA Laboratories Division,
Princeton, N. J.

Summary

The scintillation type nuclear radiation detector represents an extremely important advance and holds promise of displacing the older types of detectors for many applications. It depends for its operation on the conversion into an electrical pulse of the light flash produced by a suitable phosphor crystal when the latter absorbs a nuclear particle such as an alpha, beta or gamma ray, or neutron. The conversion of the light flash is effected by means of a secondary emission multiplier.

The present paper gives the results of the examination of a number of RCA 931A type multipliers for their suitability for this application. The properties of interest are (1) the pulse performance of the multiplier under conditions such that individual, or at most only a few, photoelectrons from the photocathode contribute to the pulse, and (2) the number and distribution of spurious pulses generated by the multiplier in darkness.

It was found that the pulse height distribution at the output of a multiplier, due to pulses from individual photoelectrons, is considerably broader than would be expected from a Poisson's distribution of secondary electrons at each stage. Distribution curves are given.

In complete darkness a good multiplier at room temperature is found to produce 300 to 600 pulses per second with a height equal to or greater than the charge on an electron times the average gain of the tube. Curves are given of dark current pulse distributions, the effect of temperature, shield potentials, etc.

(11 pages; 8 figures)

* Decimal Classification: (R800) 535.38.

† *RCA Review*, December, 1948.

APPENDIX I

ELECTRON TUBES

A Bibliography of Technical Papers

by RCA Authors

(1942-1948)

This listing includes some 170 technical papers on electron tubes, thermionics, and related subjects, selected from those written by RCA Authors and published during the period 1942-1948.

Papers are listed chronologically except in cases of multiple publication. Papers which have appeared in more than one journal are listed once, with additional publication data appended.

Abbreviations used in listing the various journals are given on the following pages.

Any requests for copies of papers listed herein should be addressed to the publication to which credited. However, *RCA Licensee Bulletins* are not published and are issued only as a service to licensees of the Radio Corporation of America.

ABBREVIATIONS

(Note—Titles of periodicals not listed below, as well as book titles, are not abbreviated.)

<i>Amer. Jour. Phys.</i>	AMERICAN JOURNAL OF PHYSICS
<i>Amer. Rev.</i>	AMERICAN REVIEW
<i>An. Amer. Acad. Polit. Soc. Sci.</i> ..	ANNALS OF THE AMERICAN ACADEMY OF POLITICAL AND SOCIAL SCIENCES
<i>ASTM Bulletin</i>	BULLETIN OF THE AMERICAN SOCIETY FOR TESTING MATERIALS
<i>Broad. Eng. Jour.</i>	BROADCAST ENGINEERS JOURNAL (A.T.E. JOURNAL)
<i>Comm. and Broad. Eng.</i>	COMMUNICATION AND BROADCASTING ENGINEERING
<i>Elec. Eng.</i>	ELECTRICAL ENGINEERING (TRANSACTIONS A.I.E.E.)
<i>Electronic Ind.</i>	ELECTRONIC INDUSTRIES
<i>FM and Tele.</i>	FM AND TELEVISION
<i>G.E. Review</i>	GENERAL ELECTRIC REVIEW
<i>ICS</i>	INTERNATIONAL CORRESPONDENCE SCHOOLS
<i>Ind. Eng. Chem.</i>	INDUSTRIAL AND ENGINEERING CHEMISTRY
<i>Ind. Standard.</i>	INDUSTRIAL STANDARDIZATION (AMERICAN STANDARDS ASSOCIATION JOURNAL)
<i>Inter. Project</i>	INTERNATIONAL PROJECTIONIST
<i>Jour. Acous. Soc. Amer.</i>	JOURNAL OF THE ACOUSTICAL SOCIETY OF AMERICA
<i>Jour. A.I.E.E.</i>	JOURNAL OF THE AMERICAN INSTITUTE OF ELECTRICAL ENGINEERS
<i>Jour. Appl. Phys.</i>	JOURNAL OF APPLIED PHYSICS
<i>Jour. Amer. Ceramic Soc.</i>	JOURNAL OF THE AMERICAN CERAMIC SOCIETY
<i>Jour. Amer. Concrete Inst.</i>	JOURNAL OF THE AMERICAN CONCRETE INSTITUTE
<i>Jour. Amer. Pharmaceutical Assoc.</i>	JOURNAL OF THE AMERICAN PHARMACEUTICAL ASSOCIATION
<i>Jour. Bacteriology</i>	JOURNAL OF BACTERIOLOGY
<i>Jour. British Inst. Cine.</i>	JOURNAL OF THE BRITISH INSTITUTE OF CINEMATICS
<i>Jour. Chem. Phys.</i>	JOURNAL OF CHEMICAL PHYSICS
<i>Jour. Eng. Educ.</i>	JOURNAL OF ENGINEERING EDUCATION
<i>Jour. Frank. Inst.</i>	JOURNAL OF THE FRANKLIN INSTITUTE
<i>Jour. Opt. Soc. Amer.</i>	JOURNAL OF THE OPTICAL SOCIETY OF AMERICA
<i>Jour. Sci. Inst. (Brit.)</i>	JOURNAL OF SCIENTIFIC INSTRUMENTS (BRITISH)
<i>Jour. Soc. Mot. Pic. Eng.</i>	JOURNAL OF THE SOCIETY OF MOTION PICTURE ENGINEERS
<i>Jour. Tele. Soc. (Brit.)</i>	JOURNAL OF THE TELEVISION SOCIETY (BRITISH)

ABBREVIATIONS (Continued)

<i>Phys. Rev.</i>	PHYSICAL REVIEW
<i>Proc. Amer. Phil. Soc.</i>	PROCEEDINGS OF THE AMERICAN PHILOSOPHICAL SOCIETY
<i>Proc. I.R.E.</i>	PROCEEDINGS OF THE INSTITUTE OF RADIO ENGINEERS
<i>Proc. Nat. Elec. Conf.</i>	PROCEEDINGS OF THE NATIONAL ELECTRONICS CONFERENCE
<i>Proc. Rad. Club Amer.</i>	PROCEEDINGS OF THE RADIO CLUB OF AMERICA
<i>Product Eng.</i>	PRODUCT ENGINEERING
<i>Project. Eng.</i>	PROJECTION ENGINEERING
<i>Project. Jour. (Brit.)</i>	PROJECTIONISTS JOURNAL (BRITISH)
<i>QST</i>	QST (A.R.R.L.)
<i>Radio and Tele.</i>	RADIO AND TELEVISION
<i>Radio Eng.</i>	RADIO ENGINEERING
<i>Radio Tech. Digest</i>	RADIO TECHNICAL DIGEST
<i>RCA Rad. Serv. News</i>	RCA RADIO SERVICE NEWS
<i>Rev. Mod. Phys.</i>	REVIEWS OF MODERN PHYSICS
<i>Rev. Sci. Instr.</i>	REVIEW OF SCIENTIFIC INSTRUMENTS
<i>RMA Eng.</i>	RMA ENGINEER
<i>Sci. Monthly</i>	SCIENTIFIC MONTHLY
<i>Sci. News Ltr.</i>	SCIENCE NEWS LETTER
<i>Short Wave and Tele.</i>	SHORT WAVE AND TELEVISION
<i>TBA Annual</i>	ANNUAL OF THE TELEVISION BROADCASTERS ASSOCIATION
<i>Teleg. & Teleph. Age</i>	TELEGRAPH AND TELEPHONE AGE
<i>Tele. News</i>	TELEVISION NEWS
<i>The T & R Bulletin (Brit.)</i>	BULLETIN OF THE RADIO SOCIETY OF GREAT BRITAIN
<i>Trans. Amer. Soc. Mech. Eng.</i>	TRANSACTIONS OF THE AMERICAN SOCIETY OF MECHANICAL ENGINEERS
<i>Trans. Electrochem. Soc.</i>	TRANSACTIONS OF THE ELECTRO-CHEMICAL SOCIETY

ELECTRON TUBE BIBLIOGRAPHY

	Year
“An Analysis of the Signal-to-Noise Ratio of U-H-F Receivers”, E. W. Herold, <i>RCA Review</i> (January)	1942
“The Absolute Sensitivity of Radio Receivers”, D. O. North, <i>RCA Review</i> (January)	1942
“The Design and Development of Three New Ultra-High-Frequency Transmitting Tubes”, C. E. Haller, <i>Proc. I.R.E.</i> (January)	1942
“Factors Governing Performance of Electron Guns in Television Cathode-Ray Tubes”, R. R. Law, <i>Proc. I.R.E.</i> (February)	1942
“The Operation of Frequency Converters and Mixers for Superheterodyne Reception”, E. W. Herold, <i>Proc. I.R.E.</i> (February)	1942
“Formulas for the Amplification Factor for Triodes—1”, B. Salzberg, <i>Proc. I.R.E.</i> (March)	1942
“Low-Frequency Characteristics of the Coupling Circuits of Single and Multi-Stage Video Amplifiers”, H. L. Donley and D. W. Epstein, <i>RCA Review</i> (April)	1942
“Sealing Mica to Glass or Metal to Form a Vacuum-Tight Joint”, J. S. Donal, Jr., <i>Rev. Sci. Instr.</i> (June)	1942
“The Relative Sensitivities of Television Pick Up Tubes Photographic Film, and the Human Eye”, Albert Rose, <i>Proc. I.R.E.</i> (June)	1942
“A Diffraction Adapter for the Electron Microscope”, J. Hillier, R. F. Baker and V. K. Zworykin, <i>Jour. Appl. Phys.</i> (September)	1942
“A Scanning Electron Microscope”, V. K. Zworykin, J. Hillier and R. L. Snyder, <i>ASTM</i> (August)	1942
“Variation of the Axial Aberrations of Electron Lenses with Lens Strength”, E. G. Ramberg, <i>Jour. Appl. Phys.</i> (September)	1942
“The RCA Electron Microscope”, J. Hillier, <i>Science Education</i> (October, November)	1942
“Vacuum Tubes—Part I”, C. Radius, <i>Radio</i> (December)	1942
“Vacuum Tubes—Part II”, C. Radius, <i>Radio</i> (January)	1943
“Vacuum Tubes—Part III”, C. Radius, <i>Radio</i> (February)	1943
“Compact 50 KW Power Amplifier”, R. F. Guy, <i>Electronic Ind.</i> (April)	1943
“R-F Operated High-Voltage Supplies for Cathode-Ray Tubes”, O. H. Schade, <i>Proc. I.R.E.</i> (April)	1943
“A Type of Light Valve for Television Reproduction”, J. S. Donal, Jr. and D. B. Langmuir, <i>Proc. I.R.E.</i> (May)	1943
“Cathode-Ray Control of Television Light Valves”, J. S. Donal, Jr., <i>Proc. I.R.E.</i> (May)	1943
“Analysis of Rectifier Operation”, O. H. Schade, <i>Proc. I.R.E.</i> (July)	1943
“Some Aspects of Radio Reception at U-H-F, Part II—Admittances and Fluctuation Noise of Tubes and Circuits”, E. W. Herold and L. Malter, <i>Proc. I.R.E.</i> (September)	1943
“Some Aspects of Radio Reception at U-H-F, Part III—Signal-to-Noise Ratio of Radio Receivers”, E. W. Herold and L. Malter, <i>Proc. I.R.E.</i> (September)	1943
“Space-Current Flow in Vacuum-Tube Structures”, B. J. Thompson, <i>Proc. I.R.E.</i> (September)	1943
“Some Aspects of Radio Reception at U-H-F, Part IV—General Superheterodyne Considerations at U-H-F”, E. W. Herold and L. Malter, <i>Proc. I.R.E.</i> (October)	1943
“Some Aspects of Radio Reception at U-H-F, Part V—Frequency Mixing in Diodes”, E. W. Herold and L. Malter, <i>Proc. I.R.E.</i> (October)	1943
“On Microanalysis by Electrons”, J. Hillier, <i>Phys. Rev.</i> (November)	1943
“A Compact High Resolving Power Electron Microscope”, V. K. Zworykin and J. Hillier, <i>Jour. Appl. Phys.</i> (December)	1943
“Electron Bombardment in Television Tubes”, I. G. Maloff, <i>Electronics</i> (January)	1944
“The Multivibrator—Applied Theory and Design—Part I”, E. R. Shenk, <i>Electronics</i> (January)	1944

	Year
"The Multivibrator—Applied Theory and Design—Part II", Eugene R. Shenk, <i>Electronics</i> (February)	1944
"The Multivibrator—Applied Theory and Design—Part III", E. R. Shenk, <i>Electronics</i> (March)	1944
"Phosphors for Electron Tubes", H. W. Leverenz, <i>Radio News</i> (April)	1944
"Using Electron for Microanalysis", V. K. Zworykin, <i>Science</i> (April 28)	1944
"Frequency Modulation of Resistance-Capacitance Oscillators", Maurice Artzt, <i>Proc. I.R.E.</i> (July)	1944
"Grounded-Grid Radio-Frequency Voltage Amplifiers", M. C. Jones, <i>Proc. I.R.E.</i> (July)	1944
"The Iconoscope", B. W. Southwell, <i>QST</i> (July)	1944
"Automatic Frequency Control of Synchronization in Television", <i>RCA Licensee Bulletin LB-624</i> (August 31)	1944
"Microanalysis by Means of Electrons", J. Hillier and R. F. Baker, <i>Jour. Appl. Phys.</i> (September)	1944
"Studies With the Electron Microscope Diffraction Adapter", R. G. Picard, <i>Jour. Appl. Phys.</i> (September)	1944
"Electron Microscopes", P. C. Smith and R. G. Picard, <i>Radio News</i> (November)	1944
"The Electron Microscope", V. K. Zworykin, J. Hillier and A. W. Vance, <i>Medical Physics</i>	1944
"Cathode Coupled Wide-Band Amplifiers", <i>RCA Licensee Bulletin LB-631</i> (January 4)	1945
"Improved Electron Gun for Cathode-Ray Tubes", L. E. Swedlund, <i>Electronics</i> (March)	1945
"RCA Electron Microscopes", P. C. Smith, <i>Jour. Eng. Educ.</i> (March)	1945
"Practical Design of Video Amplifiers—Part I", E. A. Henry, <i>QST</i> (April)	1945
"The Photoconductivity of Zinc Cadmium Sulphide as Measured with the Cathode-Ray Oscillograph", A. E. Hardy, <i>Trans. Electrochem. Soc.</i> (April)	1945
"Practical Design of Video Amplifiers—Part II", E. A. Henry, <i>QST</i> (May)	1945
"The NBC Type NM-3 Multiple Amplifier", <i>NBC Eng. Notice (Apparatus)</i> No. 21 (May 21)	1945
"Thoriated-Tungsten Wire Tested by Simple Device", G. R. Feaster, <i>Sci. News Ltrs.</i> (July 21)	1945
"The Secondary Electron Emission at Pyrex Glass", C. W. Mueller, <i>Jour. Appl. Phys.</i> (August)	1945
"Conversion Loss of Diode Mixers Having Image-Frequency Impedance", E. W. Herold, R. R. Bush, and W. R. Ferris, <i>Proc. I.R.E.</i> (September)	1945
"Cathode-Coupled Wide-Band Amplifiers", G. C. Sziklai and A. C. Schroeder, <i>Proc. I.R.E.</i> (October)	1945
"The Hydrogen Gauge—An Ultra-Sensitive Device for Location of Air Leaks in Vacuum-Device Envelopes", H. Nelson, <i>Rev. Sci. Instr.</i> (October)	1945
"Video Amplifiers", J. H. Platz, <i>Broad. Eng. Jour.</i> (October)	1945
"Television Pick-up Tubes", B. W. Southwell, <i>CQ</i> (November)	1945
"High Frequency R-F Circuits for AM-FM Receivers", E. I. Anderson, <i>RCA Licensee Bulletin LB-653</i> (December 15)	1945
ELECTRON OPTICS AND THE ELECTRON MICROSCOPE, V. K. Zworykin, G. A. Morton, E. G. Ramberg, J. Hillier, and A. W. Vance, John Wiley and Sons, New York, N. Y.	1945
"On the Improvement of Resolution in Electron Diffraction Cameras", J. Hillier and R. F. Baker, <i>Jour. Appl. Phys.</i> (January)	1946
"The Grounded-Grid Amplifier", C. J. Starner, <i>Broadcast News</i> (January)	1946
"The Electron Gun", B. W. Southwell, <i>CQ</i> (February)	1946

	Year
“A New Exciter Unit for Frequency Modulated Transmitters”, N. J. Oman, <i>RCA Review</i> (March)	1946
“Improved Cathode-Ray Tubes with Metal-Backed Luminescent Screens”, D. W. Epstein and L. Pensak, <i>RCA Review</i> , (March) ..	1946
“Induction Heating in Radio Electron-Tube Manufacture”, E. E. Spitzer, <i>Proc. I.R.E.</i> (March)	1946
“Quantum Effects in the Interaction of Electrons with High Frequency Fields and the Transmission to Classical Theory”, L. P. Smith, <i>Phys. Rev.</i> (March 1 and 15)	1946
“Input Impedance of Several Receiving-Type Pentodes at F-M and Television Frequencies”, F. Mural, <i>RCA Licensee Bulletin LB-661</i> (March 15)	1946
“Frequency Converter Considerations at 100 Mc.”, H. A. Finke, and A. A. Barco, <i>RCA Licensee Bulletin LB-665</i> (March 25)	1946
“Further Improvement in the Resolving Power of the Electron Microscope”, J. Hillier, <i>Jour. Appl. Phys.</i> (April)	1946
“Grounded-Grid Power Amplifiers”, E. E. Spitzer, <i>Electronics</i> (April) ..	1946
“Superheterodyne Frequency Conversion Using Phase-Reversal Modulation”, E. W. Herold, <i>Proc. I.R.E.</i> (April)	1946
“A Phototube for Dye Image Sound Track”, A. M. Glover and A. R. Moore, <i>Jour. Soc. Mot. Pic. Eng.</i> (May)	1946
“Behavior of a New Blue-Sensitive Phototube in Theater Sound Equipment”, J. D. Phyfe, <i>Jour. Soc. Mot. Pic. Eng.</i> (May)	1946
“Electronic Transducers”, H. F. Olson and J. Avins, <i>RCA Licensee Bulletin LB-667</i> (May 27)	1946
“Photographic Film, Television Pick-Up Tubes and the Eye”, A. Rose, <i>Inter. Project.</i> (May)	1946
“Resonant-Cavity Measurements”, R. L. Sproull and E. G. Linder, <i>Proc. I.R.E.</i> (May)	1946
“A Study of Distortion in Electron Microscopic Projection Lenses”, J. Hillier, <i>Jour. Appl. Phys.</i> (June)	1946
“Development of Pulse Triodes and Circuit to Give One Megawatt at 600 Megacycles”, R. R. Law, D. G. Burnside, R. P. Stone, and W. B. Whalley, <i>RCA Review</i> (June)	1946
“Filament Supply in the BTA-50 F Transmitter”, T. J. Boerner, <i>Broadcast News</i> (June)	1946
“Luminescence and Tenebrescence as Applied in Radar”, H. W. Leverenz, <i>RCA Review</i> (June)	1946
“Methods of Minimizing Lead Loss in Emissivity and Resistivity Determinations”, D. B. Langmuir, <i>Jour. Appl. Phys.</i> (June)	1946
“Pulse Communication”, C. W. Hansell, <i>Electronics</i> (June)	1946
“Electron Guns for Television Application”, G. A. Morton, <i>Rev. Mod. Phys.</i> (July)	1946
“A High Vacuum Gauge and Control System”, R. G. Picard, P. C. Smith and S. M. Zollers, <i>Radio News</i> (July)	1946
“The Image Orthicon—A Sensitive Television Pickup Tube”, A. Rose, P. K. Weimer and H. B. Law, <i>Proc. I.R.E.</i> (July)	1946
“Super-sensitive Tele-Pickup Tube”, W. L. Lawrence, <i>Radio Service Dealer</i> (July)	1946
“Improved Cathode-Ray Tubes are Ready For New Product Designs”, W. H. Painter, <i>Electrical Manufacturing</i> (August)	1946
“Recent Developments in Cathode-Ray Tubes”, W. H. Painter, <i>Electrical Manufacturing</i> (August)	1946
“Wave-Guide Output Magnetrons with Quartz Transformers”, L. Malter and J. L. Moll, <i>RCA Review</i> (September)	1946
“An Infrared Image Tube and Its Military Applications”, G. A. Morton and L. Flory, <i>RCA Review</i> (September)	1946
“Infrared Image Tube”, G. A. Morton and L. E. Flory, <i>Electronics</i> (September)	1946
“RCA’s New Blue-Sensitive Phototube”, J. D. Phyfe, <i>Inter. Project.</i> (September)	1946

	Year
“Current Oscillator for Television Sweep”, G. C. Sziklai, <i>Electronics</i> (September)	1946
“Mimo-Miniature Image Orthicon”, P. K. Weimer, H. B. Law and S. V. Forgue, <i>RCA REVIEW</i> (September)	1946
“Electrons at Work in Electron Tubes”, R. S. Burnap, <i>RCA Rad. Serv. News</i> (September-October)	1946
“Stability and Frequency Pulling of Loaded Unstabilized Oscillators”, J. R. Ford and N. I. Korman, <i>Proc. I.R.E.</i> (October)	1946
“A Unified Approach to the Performance of Photographic Film, Television Pickup Tubes, and the Human Eye”, A. Rose, <i>Jour. Soc. Mot. Pic. Eng.</i> (October)	1946
“Grounded-Grid Power Amplifiers”, E. E. Spitzer, <i>Broadcast News</i> (October)	1946
“Stem Electrolysis Phenomena in Soft-glass Rectifier Tubes”, John Gallup, <i>Jour. Amer. Ceramic Soc.</i> (October)	1946
“Stagger-Tuned I.F. Amplifiers”, A. Newton and R. S. Mautner, <i>RCA Licensee Bulletin LB-682</i> , (October 1)	1946
“The Universal Electron Microscope as a High Resolution Diffraction Camera”, R. G. Picard and J. H. Reisner, <i>Rev. Sci. Instr.</i> (November)	1946
“An M-Type Band Pass Television Amplifier”, F. Mural, <i>RCA Licensee Bulletin LB-687</i> , (November 7)	1946
“Luminescent and Tenebrescent Materials”, H. W. Leverenz, Section of <i>COMMUNICATION HANDBOOK</i> (Pender-McIlwain) J. Wiley and Sons, New York, N. Y.	1946
“Some Practical Aspects of Electron Microscopy”, V. K. Zworykin and J. Hillier, <i>Colloid Chemistry</i>	1946
“Carbide Structures in Carburized Thoriated-Tungsten Filaments”, C. W. Horsting, <i>Jour. Appl. Phys.</i> (January)	1947
“The Magnetic Electron Microscope Objective: Contour Phenomena and the Attainment of High Resolving Power”, J. Hillier and E. G. Ramberg, <i>Jour. Appl. Phys.</i> (January)	1947
“Automatic Frequency-Phase Control in TV Receivers”, A. Wright, <i>Tele-Tech</i> (February)	1947
“Input Circuit Noise Calculations for F-M and Television Receivers”, W. J. Stolze, <i>Communications</i> (February)	1947
“A Coaxial-Line Diode Noise Source for U-H-F”, H. Johnson, <i>RCA Review</i> (March)	1947
“Determination of Current and Dissipation Values for High-Vacuum Rectifier Tubes”, A. P. Kauzmann, <i>RCA Review</i> (March)	1947
“Excess Noise in Cavity Magnetrons”, R. L. Sproull, <i>Jour. Appl. Phys.</i> (March)	1947
“The Maximum Efficiency of Reflex-Klystron Oscillators”, E. G. Linder and R. L. Sproull, <i>Proc. I.R.E.</i> (March)	1947
“Mechano-Electronic Transducers”, H. F. Clson, <i>Jour. Acous. Soc. Amer.</i> (March)	1947
“Power Measurements of Class B Audio Amplifier Tubes”, D. P. Heacock, <i>RCA Review</i> (March)	1947
“The Present Status and Future Possibilities of the Electron Microscope”, J. Hillier, <i>RCA Review</i> (March)	1947
“Television High Voltage R-F Supplies”, R. S. Mautner and O. H. Schade, <i>RCA Review</i> (March)	1947
“The Electron Mechanics of Induction Acceleration”, J. A. Rajchman and W. H. Cherry, <i>Jour. Frank. Inst.</i> , Part I (April)	1947
Part II (May)	1947
“Some New Aspects of Germanate and Fluoride Phosphors”, F. E. Williams, <i>Jour. Opt. Soc. Amer.</i> (April)	1947
“Input Admittance of Receiving Tubes”, <i>RCA Application Note AN-118</i> , RCA Tube Department, Harrison, N. J. (April 15)	1947
“The Mechanism of the Luminescence of Solids”, F. E. Williams (Co-author), <i>Jour. Chem. Phys.</i> (May)	1947

	Year
“Use of the 2E24 and 2E26 at 162 Megacycles”, <i>RCA Application Note AN-119</i> , RCA Tube Department, Harrison, N. J. (May 15)	1947
“Coaxial Tantalum Cylinder Cathode for Continuous-Wave Magnetrons”, R. L. Jepsen, <i>RCA Review</i> (June)	1947
“Image Orthicon Field Equipment”, J. H. Roe, <i>Broadcast News</i> (June)	1947
“Miniature Tubes in War and Peace”, N. H. Green, <i>RCA Review</i> (June)	1947
“Multiplier Photo-Tube Characteristics: Application to Low Light Levels”, R. W. Engstrom, <i>Jour. Opt. Soc. Amer.</i> (June)	1947
“Stabilized Magnetron for Beacon Service”, J. S. Donal, Jr., C. L. Cuccia, B. B. Brown, C. P. Vogel and W. J. Dodds, <i>RCA Review</i> (June)	1947
“Compensation of Frequency Drift”, W. A. Harris and D. P. Heacock, <i>RCA Licensee Bulletin LB-715</i> (June 12)	1947
“Operation of the RCA-6SB7-Y Converter”, <i>RCA Application Note AN-120</i> , RCA Tube Department, Harrison, N. J. (June 16)	1947
“Use of the 6BA6 and 6BE6 Miniature Tubes in FM Receivers”, <i>RCA Application Note AN-121</i> , RCA Tube Department, Harrison, N. J. (June 16)	1947
“A Frequency-Modulated Magnetron for Super-High Frequencies”, G. R. Kilgore, C. I. Shulman, and J. Kurshan, <i>Proc. I.R.E.</i> (July)	1947
“Frequency Modulation and Control by Electron Beams”, L. P. Smith and C. I. Shulman, <i>Proc. I.R.E.</i> (July)	1947
“Generalized Theory of Multitone Amplitude and Frequency Modulation”, L. J. Giacoletto, <i>Proc. I.R.E.</i> (July)	1947
“A Newly Developed Light Modulator for Sound Recording”, G. L. Dimmick, <i>Jour. Soc. Mot. Pic. Eng.</i> (July)	1947
“Television Power Supplies”, M. Kaufman, <i>Service</i> (July)	1947
“A 1-Kilowatt Frequency-Modulated Magnetron for 900 Megacycles”, J. S. Donal, Jr., R. R. Bush, C. L. Cuccia, and H. R. Hegbar, <i>Proc. I.R.E.</i> (July)	1947
“Pulsed Rectifiers for Television Receivers”, I. G. Maloff, <i>Electronics</i> (August)	1947
“Degenerative I-F Amplifier”, R. S. Mautner and P. Neuwirth, <i>RCA Licensee Bulletin LB-722</i> (August 20)	1947
“Beam-Deflection Control for Amplifier Tubes”, G. R. Kilgore, <i>RCA Review</i> (September)	1947
“Class B Output for Automobile Receivers”, L. E. Barton and J. B. Coleman, <i>RCA Licensee Bulletin LB-726</i> (September 15)	1947
“Electrostatic Deflection for 7GP4 Kinescope”, W. Milwitt and E. Schoenfeld, <i>RCA Licensee Bulletin LB-701</i> (September 22)	1947
“The Behavior of ‘Magnetic’ Electron Multipliers as a Function of Frequency”, L. Malter, <i>Proc. I.R.E.</i> (October)	1947
“Cathode Follower Gate Circuit”, J. Kurshan, <i>Rev. Sci. Instr.</i> (September)	1947
“Compensation of Frequency Drift”, <i>RCA Application Note AN-122</i> , RCA Tube Department, Harrison, N. J. (October 15)	1947
“Receiver Microphonics Caused by Heater-Cathode Capacitance Variations”, <i>RCA Application Note AN-123</i> , RCA Tube Department, Harrison, N. J. (October 15)	1947
“The Motion of Electrons Subject to Forces Transverse to a Uniform Magnetic Field”, P. K. Weimer and A. Rose, <i>Proc. I.R.E.</i> (November)	1947
“10.7 Megacycle FM Intermediate Frequency Signal Generator”, W. R. Alexander, <i>RCA Licensee Bulletin LB-737</i> (November 10)	1947
“Blower Requirements for RCA Forced-Air-Cooled Tubes”, <i>RCA Application Note AN-125</i> , RCA Tube Department, Harrison, N. J. (November 15)	1947

	Year
“Suppression of Arc-Over, Corona, and High-Voltage Leakage in the 5TP4 Kinescope”, <i>RCA Application Note AN-124</i> , RCA Tube Department, Harrison, N. J. (November 15)	1947
“Audio Noise Reduction Circuits”, H. F. Olson, <i>Electronics</i> (December)	1947
“Performance Characteristics of Long-Persistence Cathode-Ray Tube Screens; Their Measurement and Control”, R. E. Johnson and A. E. Hardy, <i>RCA Review</i> (December)	1947
“Small-Signal Analysis of Traveling-Wave Tube”, C. I. Shulman and M. S. Heagy, <i>RCA Review</i> (December)	1947
“Storage Orthicon and Its Application to Teleran”, S. V. Forgue, <i>RCA Review</i> (December)	1947
“A Tube Complement for AC/DC AM/FM Receivers”, <i>RCA Application Note AN-127</i> , RCA Tube Department, Harrison, N. J. (January 2)	1948
“Circuit Design Precautions to Prevent Internal Arcs from Damaging Kinescopes”, <i>RCA Application Note AN-128</i> , RCA Tube Department, Harrison, N. J. (January 15)	1948
“Pulse-Operated High-Voltage Power Supply for Television Receivers”, <i>RCA Application Note AN-130</i> , RCA Tube Department, Harrison, N. J. (February 16)	1948
“Barrier Grid Storage Tube and Its Operation”, A. S. Jensen, J. P. Smith, M. H. Mesner, and L. E. Flory, <i>RCA Review</i> (March) ..	1948
“A Developmental Pulse Triode for 200 KW Output at 600 Mc.”, L. S. Nergaard, D. G. Burnside, and R. P. Stone, <i>Proc. I.R.E.</i> (March) ..	1948
“Quality Control of Miniature Tubes”, W. L. Van Keuren, <i>RCA Rad. Serv. News</i> (March-April)	1948
“Quick Changing of 8D21 Tube”, E. H. Potter, <i>Broadcast News</i> (March)	1948
“Stereoscopic Viewing of Cathode-Ray Tube Presentations”, H. Iams, R. L. Burtner, and C. H. Chandler, <i>RCA Review</i> (March)	1948
“Electronic Timers Employing Thyratrons 2D21 or 2050”, <i>RCA Application Note AN-131</i> , RCA Tube Department, Harrison, N. J. (March 1)	1948
“The Magic of Making Television Picture Tubes”, Pamphlet, RCA Department of Information, New York, N. Y. (April)	1948
“Dynamic Operating Conditions in Video Amplifiers”, Frank Mural, <i>RCA Licensee Bulletin LB-750</i> (April 20)	1948
“Clickless Keying Using V-R Tubes”, A. M. Seybold, <i>CQ</i> (May)	1948
“Note on Means of Measurement of Output Plate A. C. Voltage of a Television Deflection Circuit During Scanning Interval”, J. M. Brumbaugh, <i>Broadcast News</i> (May)	1948
“Improved Arrangement of Base-Pin Connections in New Miniature Tube Types”, <i>RCA Application Note AN-133</i> , RCA Tube Department, Harrison, N. J. (May 17)	1948
“Receiver Sensitivity and Gain Measurements at High Frequencies”, <i>RCA Application Note AN-132</i> , RCA Tube Department, Harrison, N. J. (May 17)	1948
“Versatile Noise-Reduction Amplifier”, K. Singer, <i>Jour. Soc. Mot. Pic. Eng.</i> (June)	1948
“Adjustment of Filament Voltage of RCA 1B3-GT by Observation of Filament Temperature”, <i>RCA Application Note AN-134</i> , RCA Tube Department, Harrison, N. J. (June 15)	1948
“Single-Section Filament Operation of Types 3S4 and 3V4”, <i>RCA Application Note AN-135</i> , RCA Tube Department, Harrison, N. J. (June 15)	1948
“Chromatic Aberration and Resolving Power in Electron Microscopy”, E. G. Ramberg and J. Hillier, <i>Jour. Appl. Phys.</i> (July)	1948
“Overload Protection for the Horizontal Deflection Circuit in Television Receivers”, <i>RCA Application Note AN-136</i> , RCA Tube Department, Harrison, N. J. (July 15)	1948

	Year
“Reduction in Peak Inverse Voltage Rating of Type 1B3-GT”, <i>RCA Application Note AN-137</i> , RCA Tube Department, Harrison, N. J. (July 15)	1948
“The Brightness Intensifier”, G. A. Morton, J. E. Ruedy and G. L. Krieger, <i>RCA Review</i> (September)	1948
“Some Notes on Noise Theory and its Application to Input Circuit Design”, W. A. Harris, <i>RCA Review</i> (September)	1948
“Temperature Dependence of the Emission Bands of Zinc Oxide Phosphors”, F. H. Nicoll, <i>Jour. Opt. Soc. Amer.</i> (September)	1948
“A New 100-Watt Triode for 1000 Megacycles”, W. P. Bennett, E. A. Eschbach, C. E. Haller, and W. R. Keye, <i>Proc. I.R.E.</i> (October)	1948
“Duplex Tetrode UHF Power Tubes”, P. T. Smith, H. R. Hegbar, <i>Proc. I.R.E.</i> (November)	1948
“Optimum High-Frequency Bias in Magnetic Recording”, G. L. Dimmick and S. W. Johnson, <i>Jour. Soc. Mot. Pic. Eng.</i> (November)	1948
“Analysis of a Simple Model of Two-Beam Growing-Wave Tube”, L. S. Nergaard, <i>RCA Review</i> (December)	1948
“Performance of 931-A Type Multiplier in a Scintillation Counter”, G. A. Morton and J. A. Mitchell, <i>RCA Review</i> (December)	1948
“A Technique for the Making and Mounting of Fine Mesh Screens”, H. B. Law, <i>Rev. Sci. Instr.</i> (December)	1948
“The Transitrol, An Experimental Automatic-Frequency-Control Tube”, J. Kurshan, <i>RCA Review</i> (December)	1948

APPENDIX II

LIST OF APPLICATION NOTES (1947-1948)

RCA Application Notes are published by the RCA Tube Department. The list below is included to provide a convenient additional reference source.

APPLICATION NOTES

NUMBER	YEAR	TITLE
AN-118	1947	Input Admittance of Receiving Tubes
AN-119	1947	Use of the 2E24 and 2E26 at 162 Megacycles
AN-120	1947	Operation of the RCA-6SB7-Y Converter
AN-121	1947	Use of the 6BA6 and 6BE6 Miniature Tubes in FM Receivers
AN-122	1947	Compensation of Frequency Drift
AN-123	1947	Receiver Microphonics Caused by Heater-Cathode Capacitance Variations
AN-124	1947	Suppression of Arc-Over, Corona, and High-Voltage Leakage in the 5TP4 Kinescope
AN-125	1947	Blower Requirements for RCA Forced-Air-Cooled Tubes
AN-126	1947	Use of Miniature Tubes in Stagger-Tuned Video Intermediate-Frequency Systems
AN-127	1948	A Tube Complement for AC/DC AM/FM Receivers
AN-128	1948	Circuit Design Precautions to Prevent Internal Arcs from Damaging Kinescopes
AN-129	1948	RCA Special Red Tubes for Industrial Application
AN-130	1948	Pulse-Operated High-Voltage Power Supply for Television Receivers
AN-131	1948	Electronic Timers Employing Thyratrons 2D21 or 2050
AN-132	1948	Receiver Sensitivity and Gain Measurements at High Frequencies
AN-133	1948	Improved Arrangement of Base-Pin Connections in New Miniature Tube Types
AN-134	1948	Adjustment of Filament Voltage of RCA 1B3-GT by Observation of Filament Temperature
AN-135	1948	Single-Section Filament Operation of Types 3S4 and 3V4
AN-136	1948	Overload Protection for the Horizontal Deflection Circuit in Television Receivers
AN-137	1948	Reduction in Peak Inverse Voltage Rating of Type 1B3-GT